

**DEGRADATION OF SELENOCYANATE WITH AN ADVANCED
REDUCTION PROCESS (ARP)**

A Thesis

by

GUOFAN LUO

Submitted to the Office of Graduate and Professional Studies of
Texas A&M University
in partial fulfillment of the requirements for the degree of

MASTER OF SCIENCE

Chair of Committee,	Bill Batchelor
Committee Members,	Qi Ying
	Sergio Capareda
Head of Department,	Robin Autenrieth

August 2014

Major Subject: Civil Engineering

Copyright 2014 Guofan Luo

ABSTRACT

Selenocyanate (SeCN^-) is a common form of selenium contamination in refinery and mining wastewater generated from processing oil or minerals from seleniferous formations such as marine shales. Humans who drink water containing selenium over several years may experience hair or fingernail losses and numbness in fingers or toes. Recently, advanced reduction processes (ARP) that combine chemical reductants with activating methods has been studied to decompose contaminants that have the potential to be chemically reduced.

This paper focus on the application of ARP to selenium removal from wastewater containing selenocyanate. The ARP in this study consists of ferrous iron (chemical reductant) and UV light (activating method). During this research, control experiments were conducted to see the individual reactions of selenocyanate alone, selenocyanate with ferrous iron, and selenocyanate with UV light. Also, the effect of pH and UV light irradiance were studied.

The results show that the ferrous iron alone cannot improve selenocyanate removal. However, UV light is able to degrade selenocyanate, and the reaction rate increases as pH decreases. The ARP in this system (ferrous iron and UV) cannot improve the reaction rate from that of only UV light, but the addition of ferrous iron did decrease the final concentration of selenium at high pH.

DEDICATION

I would like to dedicate this thesis to my parents, who always love and support me, and encourage me to face the difficulties under all circumstances.

ACKNOWLEDGEMENTS

I would like to thank my committee chair, Dr. Batchelor, who always had time for me, and taught me so much in every aspect of science, from experimental design to data analysis, from critical thinking to scientific writing. I could not have asked for a better supervisor. Also, thanks to my committee members, Dr. Ying and Dr. Capareda, for their guidance and support throughout the course of this research.

Thanks also go to my friends and colleagues and the department faculty and staff for making my time at Texas A&M University a great experience.

Finally, thanks to my mother and father for their encouragement and to my girlfriend for her patience and love.

TABLE OF CONTENTS

	Page
ABSTRACT	ii
DEDICATION	iii
ACKNOWLEDGEMENTS	iv
TABLE OF CONTENTS	v
LIST OF FIGURES.....	vii
LIST OF TABLES	ix
1. INTRODUCTION.....	1
2. BACKGROUND.....	3
2.1 Selenocyanate.....	3
2.1.1 Physical and chemical properties of selenocyanate	3
2.1.2 Source.....	5
2.1.3 Toxicity	6
2.1.4 Current treatment methods	7
2.2 Advanced reduction process.....	9
2.2.1 Ultraviolet light	9
2.2.2 Ferrous iron	10
3. METHODOLOGY	13
3.1 Equipment and regents	13
3.1.1 Anaerobic chamber.....	13
3.1.2 Reagents	13
3.1.3 Apparatus.....	14
3.2 Experimental procedures.....	14
3.2.1 Solution preparation	14
3.2.2 Experiment plan	15
3.2.2.1 Effect of pH.....	15
3.2.2.2 Effect of UV light irradiance.....	16
3.2.2.3 Effect of ferric iron's existing form	16
3.2.3 Sampling.....	16
3.3 Analytical procedures.....	17
3.3.1 Qualitative analysis	17
3.3.2 Quantitative analysis	17

	Page
4. RESULTS AND DISCUSSION	23
4.1 Experiments of effect on pH	23
4.1.1 Blank control	23
4.1.2 Reagent control.....	26
4.1.3 Light control	28
4.1.4 ARP experiments (ferrous iron + UV light).....	36
4.2 Experiments of effect on light irradiance	42
4.3 Experiments of effect on ferric iron	47
5. CONCLUSION	49
6. RECOMMENDATION	51
REFERENCES	52

LIST OF FIGURES

	Page
Figure 3.1 ICP-MS system	18
Figure 3.2 Valve system.....	20
Figure 3.3 Example standard curve.....	21
Figure 4.1 Soluble selenium concentrations over time at pH = 4 (blank control, initial selenocyanate as selenium = 0.71 mg/L).....	24
Figure 4.2 Soluble selenium concentrations over time at pH = 7 (blank control, initial selenocyanate as selenium = 0.95 mg/L).....	25
Figure 4.3 Soluble selenium concentrations over time at pH = 10 (blank control, initial selenocyanate as selenium = 0.98 mg/L).....	25
Figure 4.4 Soluble selenium concentrations over time at pH = 4 (reagent control, ferrous iron = 10 mg/L, initial selenocyanate as selenium = 0.69 mg/L)	27
Figure 4.5 Soluble selenium concentrations over time at pH = 7 (reagent control, ferrous iron = 10 mg/L, initial selenocyanate as selenium = 0.78 mg/L)	27
Figure 4.6 Soluble selenium concentrations over time at pH = 10 (reagent control, ferrous iron = 10 mg/L, initial selenocyanate as selenium = 0.99 mg/L)	28
Figure 4.7 Soluble selenium concentrations over time at pH = 4 (light control, UV irradiance = 5000 $\mu\text{W}/\text{cm}^2$, initial selenocyanate as selenium = 0.98 mg/L).....	29
Figure 4.8 Soluble selenium concentrations over time at pH = 7 (light control, UV irradiance = 5000 $\mu\text{W}/\text{cm}^2$, initial selenocyanate as selenium = 0.97 mg/L).....	29
Figure 4.9 Soluble selenium concentrations over time at pH = 10 (light control, UV irradiance = 5000 $\mu\text{W}/\text{cm}^2$, initial selenocyanate as selenium = 0.99 mg/L).....	30
Figure 4.10 UV Light absorption of selenocyanate solution	31
Figure 4.11 UV light absorbance of selenocyanate solution over time at pH = 7 (UV irradiance = 5000 $\mu\text{W}/\text{cm}^2$).....	34

	Page
Figure 4.12 Soluble selenium concentrations at three pH values during the first minute of irradiation (light control, UV irradiance = 5000 $\mu\text{W}/\text{cm}^2$)	34
Figure 4.13 Soluble selenium concentrations change over time at 3 pH values with Fe/UV-ARP (ferrous iron = 10 mg/L, UV irradiance = 5000 $\mu\text{W}/\text{cm}^2$, initial selenocyanate as selenium =1 mg/L)	37
Figure 4.14 Soluble selenium concentrations at three pH values in first minute for the Fe/UV-ARP (ferrous iron = 10 mg/L, UV irradiance = 5000 $\mu\text{W}/\text{cm}^2$)	38
Figure 4.15 Soluble selenium concentrations over time at pH = 4 (UV-Fe ARP and UV alone)	39
Figure 4.16 Soluble selenium concentrations over time at pH = 7 (UV-Fe ARP and UV alone)	40
Figure 4.17 Soluble selenium concentrations over time at pH = 10 (UV-Fe ARP and UV alone)	41
Figure 4.18 Soluble selenium concentrations over time at three values of light irradiance	44
Figure 4.19 Soluble selenium concentrations during the first minute for three values of light irradiance	44
Figure 4.20 Effect of light irradiance on initial rates	47
Figure 4.21 Soluble selenium concentrations over time at 2 pH values	48

LIST OF TABLES

	Page
Table 3.1 Instrumental operating conditions and data acquisition parameters	19
Table 3.2 Method detection limit data.....	22
Table 4.1 Initial reaction rates at different pH values	35
Table 4.2 Initial reaction rates at different pH values for UV irradiation and Fe/UV-ARP	38
Table 4.3 Initial reaction rates at different values of light irradiance	45

1. INTRODUCTION

Some refinery and mining wastewater generated from processing oil or minerals from seleniferous formations such as marine shales, contains high levels of selenocyanate (SeCN^-), which poses a great risk to humans and the environment. Many methods have been used to remove selenium from wastewater. The conventional precipitation method, including the addition of copper, is often economical, but may result in excess copper which has more restrictive criteria than selenium. Chemical processes such as oxidation of selenocyanate to selenite are also common methods; however, large amounts of COD strongly interfere with their effectiveness.

Recently, our research group has investigated Advanced Reduction Processes (ARPs) as wastewater treatment processes. ARPs combine activation methods and appropriate reductants to produce reductive free radicals. Activation methods include ultraviolet light (UV), electron beam, ultrasound and microwaves. Dithionite, sulfite, sulfide and ferrous iron are common reductants used by our group. When reductants are activated by absorbing proper energy, it can generate reactive free radicals. These free radicals may be able to break selenocyanate and help to remove selenium from wastewater.

The goal of the proposed research is to verify the ability of the Fe (II)/UV ARP to decompose selenocyanate. Three objectives are included in this research.

1. Develop experimental and analytical procedures.

2. Evaluate the effects of pH and light intensity on decomposition of selenocyanate with Fe (II)/UV ARP and determine optimal conditions for the process.
3. Characterize the kinetics of selenocyanate decomposition with Fe (II)/UV ARP by calculating of the rate constant.

2. BACKGROUND

Selenium is an element that is both essential and toxic to human beings with the effect being dependent on concentrations; a trace amount is necessary, but a high concentration should be avoided (Levander, 1987). In the environment, selenium exists in inorganic and organic forms. Inorganic forms include selenide(Se^{2-}), elemental selenium(Se^0), selenite(SeO_3^{2-}) and selenate(SeO_4^{2-}). On the other hand, selenium can form stable bonds with carbon to develop various organic selenium compounds, such as selenomethionine and benzeneselenol (Commandeur, et al. 2001). Selenium is located in the oxygen group, and its several isotopes include ^{74}Se (1.0%), ^{76}Se (9.0%), ^{77}Se (7.5%), ^{78}Se (23.5%), ^{80}Se (50.0%), ^{82}Se (9.0%) (Krouse and Thode 1961). Chemical properties of selenium and sulfur are similar with small differences in some characteristics such as oxidation potentials (McNeal and Balistreri 1989). As a result, much research on sulfur can be applied to studying selenium.

2.1 Selenocyanate

High levels of selenocyanate exist in some wastewaters at refineries that are refining crude oils from seleniferous deposits. This poses a great risk to humans and the environment. In this section, the properties, sources and toxicity of selenocyanate are discussed and some current treatment methods for selenocyanate are reviewed.

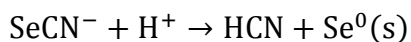
2.1.1 Physical and chemical properties of selenocyanate

Researchers started to investigate the selenocyanate salts of alkaline earth metals decades ago, and they conducted many studies about their properties. They determined

that potassium selenocyanate exists as white acicular crystal, which can deliquesce in air (Golub and Skopenko, 1965). They also found that potassium selenocyanate decomposes at a temperature of 100 °C or higher when air is present (Golub and Skopenko, 1965).

Some literature summarized selenocyanate's photoreactions. Pathem et al. (2007) observed that selenocyanate would absorb UV light at 200 nm. Kern and Hummel (1996) did some photosensitivity research on selenocyanate derivatives and they found that benzyl selenocyanate would decompose to benzyl cyanate and elemental selenium when exposed to UV light (254 nm).

Solutions of potassium selenocyanate solution are alkaline and they are not stable under acid conditions. At low pH values, selenocyanate will break down to produce elemental selenium as shown below:



The presence of some metals can activate this reaction (Golub and Skopenko 1965). Normally, potassium selenocyanate decomposes at a pH of less than 5, however, it will decompose at pH 5.5-4.9, when Na^+ , K^+ , Mg^{2+} , Ca^{2+} and Ba^{2+} exist in the solution. In the presence of Cd^{2+} , Hg^{2+} , Zn^{2+} , Pb^{2+} and Fe^{2+} , selenocyanate decomposes at $\text{pH} > 6$. Ni^+ , Co^{2+} and Cu^{2+} can start this decomposition at $\text{pH} > 7$.

Other heavy metal selenocyanates are not as soluble as potassium selenocyanate. Crooks (1851) observed that silver selenocyanate is slightly soluble. Mercury selenocyanate is sparingly soluble alone but would dissolve in the presence of iodides or cyanides (Cameron and Davy, 1881). Golub and Skopenko (1965) observed that lead selenocyanate was also sparingly soluble with saturated concentration of 0.00239 M.

Some selenocyanate complexes could be formed in aqueous solution and most of them are sparingly soluble. $KAg_2(SeCN)_3$ was obtained from potassium selenocyanate and silver selenocyanate and was stable in air and sparingly soluble in water (Golub and Skopenko, 1965). Mercury selenocyanate complexes could also be formed in aqueous solution and they were more stable than cadmium complexes (Golub and Skopenko, 1965).

2.1.2 Source

Refining crude oils produced from seleniferous deposits such as marine shale often results in high levels of selenium in the refinery wastewater and the dominant species is selenocyanate (Sandy and DiSante, 2010). Water is needed in the refining of crude oil and some of the wastewater that is produced is called “sour water”, if it contains high levels of ammonia and hydrogen sulfide. Because selenium is isomorphous with sulfur, a large amount of selenium also exists in the “sour water”. The sour water is treated with steam stripping, which decreases the ammonia and hydrogen sulfide concentration, but has little effect on selenium (Watson, 1995). As a result, selenium remains in the “treated” sour water. Miekeley et al. (2005) and Stivanin de Almeida et al. (2009) reported typical concentrations of selenium in refinery wastewater and showed that selenium exists as elemental selenium, selenite, selenate and selenocyanate, with selenocyanate being predominant in most cases. However, the forms of selenium in refinery wastewater are decided by refinery processes and other forms may also be abundant.

2.1.3 Toxicity

Selenium is a nutritionally required element for humans at low concentrations, but it becomes toxic at higher concentrations. The primary drinking water standards set by the United States Environmental Protection Agency define the maximum contaminant level goal and maximum contaminant level for selenium as 0.05 mg/l. Some people who drink water containing selenium in excess of the MCL over many years could experience hair or fingernail losses and numbness in fingers or toes (USEPA, 2011).

The selenium species that have been most investigated for their toxicity are selenate and selenite. The current recommended national water quality criterion for selenium is calculated with the formula below:

$$CMC = \left[\frac{1}{\left(\frac{f1}{CMC1}\right) + \left(\frac{f2}{CMC2}\right)} \right]$$

Where f1 and f2 are the fractions of selenite and selenate in the water, and CMC1 and CMC2 are 185.9 (selenite) and 12.82 (selenate) µg/L (USEPA, 1999). CMC is short for Criterion Maximum Concentration, which is an estimate of the highest concentration of a material in surface water to which an aquatic community can be exposed briefly without resulting in an unacceptable effect. Also, the USEPA (1999) has specified the Criterion Continuous Concentration (CCC) for selenium to be 5 µg/L.

Later, Chapman, et al. (2009) found that diet is the primary pathway of selenium exposure to aquatic species. They also found that absorbed selenium is involved in oxidation - reduction cycling, which generates reactive oxidized species that are

responsible for oxidative stress and cellular dysfunction. Also, USEPA (2004) stated that sulfate was a modifier of chronic selenate toxicity in water, because the competition for these two materials in aquatic animals. As a result, the current criterion for selenium may not be accurate.

Burra et al. (2009) concluded that toxicity of selenocyanate was comparable to that of selenite and selenate when they used the metalloid-resistant bacterium LHVE as the test organism.

2.1.4 Current treatment methods

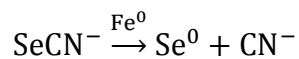
Many methods with different concepts are used to remediate selenocyanate in refinery wastewater. The most common ways are precipitation, oxidation, reduction and adsorption.

Manceau and Gallup (1997) used sodium thiosulfate and sulfites to reduce cupric ions to cuprous ions, which promoted co-precipitation that generated $\text{Cu}(\text{S}_{0.91}\text{Se}_{0.09})\text{CN}(\text{s})$. After filtration to remove the solid, caustic soda or sodium sulfide can be added to precipitate the excess copper. They also concluded that the efficiency of selenium removal with cupric ions could reach as high as 95%, when pH value was about 9. However, the more excess copper is added, the more difficult it is to remove the excess copper. Another issue associated with this method is that it is hard to consistently achieved high selenium removal in the effluent (Sandy and DiSante, 2010).

Selenocyanate can also be converted by redox reactions into forms that are more easily removed. Chlorine dioxide and hydrogen peroxide can oxidize selenocyanate to selenite, which is easy to adsorb and remove. Overman (2000) obtained a patent for

oxidizing selenocyanate to selenite by potassium permanganate at a pH range of 4.0 to 4.2. Then, the selenite can be adsorbed onto ferric hydroxide or similar insoluble materials that are suspended in water. So far, the primary difficulty in applying an oxidation method for selenium is the large amount of COD existing in refinery wastewater, which can react with oxidants resulting in the need for high doses that increase cost and make the cost of oxidizing selenium prohibitive (Sandy and DiSante, 2010). Also, the oxidizing process would result to other selenium species such as selenite and selenate, which were hard to remove as well.

On the other hand, reductants such as zero valent iron (ZVI) can also be applied to remove selenocyanate. Meng et al. (2002) found that selenocyanate reacts with ZVI rapidly to produce elemental selenium:



Iron particles can be activated at low pH, because the surface iron oxides of ZVI are removed under acidic conditions. At the same time, selenocyanate decomposes to form elemental selenium at pH lower than 5, which leads to the rate of selenocyanate removal increasing as pH decreases. Then, the elemental selenium could be easily filtered. This method suggests that it is possible to use a reduction method to decompose selenocyanate and produce solid elemental selenium that could easily be filtered.

Some redox reactions of selenocyanate are important in its behavior during wastewater treatment at refineries, which is usually accomplished by biological treatment using the activated sludge process. Activated sludge treatment at refineries oxidizes selenocyanate to selenite and selenate in the aeration tank along with large

amounts of BOD. However, without other steps, the selenite and selenate would pass out in the effluent. If there is a nitrogen removal process after conventional activated sludge treatment, these soluble selenium species could be reduced to elemental selenium in the anoxic tank and be removed in the clarifier, but this has not been demonstrated at commercial scale (Sandy and DiSante, 2010).

2.2 Advanced reduction process

Advanced reduction processes (ARPs) are combinations of a reductant with various activating methods to produce highly reactive reducing radicals that have the ability to degrade some target contaminants. For this research, we will use ultraviolet light as the activating method and ferrous iron as the reagent in the Fe(II)/UV advanced reduction process. The reactive aqueous electron produced by irradiation of Fe(II) may be an alternative to ZVI and decompose selenocyanate to elemental selenium.

2.2.1 Ultraviolet light

Ultraviolet light irradiation is a widely used disinfection technology, since it is effective against all waterborne pathogens (Hijnen et al., 2006). Also, UV-assisted processes, such as advanced oxidation processes, have been applied for treatment of organic pollutants. Li et al. (2010) degraded clofibric acid with UV/H₂O₂ process, and showed the degradation is strongly related to the presence of hydroxyl radicals (\bullet OH). As a result, UV light can be used as a source of external energy that can be absorbed by some chemicals to break bonds and yield free radicals.

Experiments have shown that UV light can be absorbed by selenocyanate (Pathem et al., 2007). Meanwhile, many studies have been conducted to investigate the

photochemistry of thiocyanate with UV. Dogliotti and Hayon (1968) pointed out that in the presence of UV, turbidity was noticeable in thiocyanate solution, indicating the formation of elemental sulfur solids. Luria and Treinin (1968) also reported that UV can be efficiently utilized to break the weak S-C bond in thiocyanate to form elemental sulfur and cyanide.



At the same time, they found that the highest reaction rate happened at first, then it decreased over time. This is due to the absorption and refraction of UV light caused by sulfur being formed, and also by fast reverse reaction that re-forms thiocyanate.

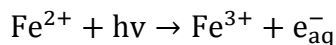
Because selenocyanate (SeCN^-) is isomorphous with thiocyanate (SCN^-), and selenocyanate can also absorb UV, it is reasonable to assume that UV treatment can be used to decompose selenocyanate into elemental selenium. This could be combined with a solids separation step such as filtration to provide a method for removing selenium from water.

2.2.2 Ferrous iron

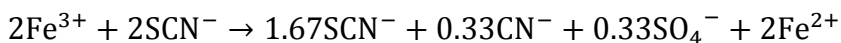
Ferrous iron is often used as a reductant. Murphy (1988) and Sedlak and Chan (1997) used ferrous iron to reduce selenate and hexavalent chromium. They found that the ferrous iron reduction potential was strongly related with pH and it would increase as pH increased. Ehrenreich and Widdel (1994) also confirmed this relationship, they found that $\text{Fe}^{3+}/\text{Fe}^{2+}$ pair has an E_o' of + 0.77 V in acidic solutions; however, the relevant

redox pair at pH 7 in bicarbonate-containing environments is $\text{Fe}(\text{OH})_3 + \text{HCO}_3^- / \text{FeCO}_3$ and it has an E_o' of + 0.2 V.

In the presence of UV, the aqueous electron will be produced in ferrous ion solutions (Airey and Dainton 1966).



The aqueous electron is a highly reactive product that can be used as a reductant. Because selenocyanate can be degraded by ZVI in a reduction process and UV can stimulate ferrous iron to produce a strong reductant, the Fe(II)/UV ARP may be able to degrade selenocyanate. In addition, the produced ferric iron may also have a positive effect on the removal of selenium. Firstly, ferric iron may react with selenocyanate. Betts and Dainton (1953) claimed that ferric iron would oxidize thiocyanate, and they gave the reaction as:



So it is reasonable to assume that ferric iron may also react with selenocyanate and form other selenium species. Secondly, in alkaline conditions, ferric iron can form ferric hydroxides, which is a very good adsorbent to remove selenocyanate from the solution.

In summary, UV may be absorbed and utilized to break the weak Se-C bond alone to produce elemental selenium. Meanwhile, the aqueous electron produced from Fe(II)/UV ARP may be able to degrade selenocyanate to elemental selenium. At the same time, the formed ferric iron may also react with selenocyanate directly or form ferric hydroxides to adsorb selenocyanate. Through either path, elemental selenium may

be produced, or selenium may be adsorbed. Elemental selenium and ferric hydroxides would be present as solid phases that could be easily filtered from the solution. Overall, there is a strong possibility that selenocyanate can be removed with the Fe(II)/UV ARP.

3. METHODOLOGY

In this chapter, all the equipment and reagents needed in the study are listed in detail and the experimental procedures are described.

3.1 Equipment and reagents

3.1.1 Anaerobic chamber

All solution preparation and irradiation experiments were conducted in an anaerobic chamber (Coy Laboratory Products Inc.). The chamber is filled with a gas mixture (95% nitrogen and 5% hydrogen) and equipped with an oxygen and hydrogen analyzer, and a palladium catalyst STAK-PAK (Coy Laboratory Products Inc.). This catalyst promotes the reaction of hydrogen with oxygen to insure low concentrations of oxygen in the chamber.

3.1.2 Reagents

The following reagents were used: potassium selenocyanate (reagent grade, 97%, Sigma-Aldrich), iron (II) chloride tetrahydrate (reagent grade, 99.0–103.0%, J.T. Baker), iron (III) chloride hexahydrate (reagent grade, 98%, Sigma-Aldrich), nitric acid (ACS grade, BDH), potassium hydrogen phosphate, potassium dihydrogen phosphate, potassium phosphate (97%, Alfa Aesar).

The deionized water (Milli-Q, Millipore) used in all experiments was deoxygenated by sparging with ultra-high purity(UHP) nitrogen for 4 hours and then sparging with a gas mixture (95% nitrogen and 5% hydrogen) for 24 hours.

3.1.3 Apparatus

All experiments were carried out in 17-ml, cylindrical, UV-transparent, quartz reactors (50 mm exterior diameter and 10 mm light path length (Sterna Cells, Inc.). The UV light source was a Phillips TUV PL-L36W/4P lamp, which emits short-wave UV radiation with a peak at 254 nm. A reaction area established in the anaerobic chamber and an UV-L lamp (254 nm) was set on the top of reaction area. A lab scissor lift was used to adjust the distance between the lamp and reactors and the light irradiance was controlled in this way. Analysis equipment were Spectronic Holios Gamma UV-Vis Spectrophotometer (Thermo scientific) and Inductively Coupled Plasma-Mass Spectrometry (Perkin Elmer, NexIon 300D).

3.2 Experimental procedures

3.2.1 Solution preparation

Selenocyanate stock solution: Potassium selenocyanate powder was sealed with parafilm, stored in the fume hood and covered with aluminum foil, in order to avoid any photoreaction. 0.1825g potassium selenocyanate was weighed and transferred into the anaerobic chamber. Then, 100 ml deoxygenated deionized water was added and mixed well with selenocyanate powder. Finally, the solution was covered with aluminum foil. The stock solution is 1000 mg/l as selenium (12.7 mmol/L).

Ferric and ferrous iron stock solutions: ferric and ferrous iron chloride powders were stored in a vacuum dryer. 0.3422 g ferric chloride hexahydrate and 0.2517 g ferrous chloride tetrahydrate were separately weighed and transferred to the centrifugal tube and placed in the anaerobic chamber. Then 100 ml deoxygenated deionized water

was added to each to obtain concentrations of 12.7 mmol/L Fe^{2+} and 12.7 mmol/L Fe^{3+} . The fresh stock solutions were prepared for each set of experiments and they were used immediately.

3.2.2 Experiment plan

Batch experiments were conducted to evaluate the effects of pH and light irradiance and ferric iron concentration on decomposition of selenocyanate. The initial concentration of selenocyanate was 1 mg/L as Se (0.0127 mmol/L), ferrous and ferric iron concentrations in the samples (0.127 mmol/L) were ten times that of selenocyanate, and their concentrations were kept constant for all the experiments in which they were present.

3.2.2.1 Effect of pH

The objective of these experiments was to investigate the effect of pH on decomposition of selenocyanate in the presence of UV light (254 nm) and ferrous iron. Batch experiments were conducted at 3 pH values (pH 4, 7, 10). At each pH value, a blank control experiment was conducted with no reductant (Ferrous iron) and no UV light. Then a reagent control experiment was conducted with ferrous iron at 10 times the concentration of selenocyanate but no UV light. Thirdly, a light control experiment was conducted with UV light (254 nm) at 5000 $\mu\text{W}/\text{cm}^2$ but no ferrous iron. Finally, the experiment with both ferrous iron (0.127 mmol/L as Fe^{2+}) and UV light (5000 $\mu\text{W}/\text{cm}^2$) was conducted. A phosphate buffer was used in all experiments to maintain pH. The buffer concentration is 10 mmol/L as PO_4^{3-} .

3.2.2.2 Effect of UV light irradiance

The objective of these experiments was to investigate the effect of UV (254 nm) light irradiance of the decomposition of selenocyanate. Batch experiments were conducted at 3 values of light irradiance (3000, 5000 and 7000 $\mu\text{W}/\text{cm}^2$), pH was fixed at 7 and no ferrous and ferric iron were involved in this set of experiments. Also, a blank experiment at pH 7 with no UV irradiation was conducted at the same time. All the experiments were conducted in the chamber.

3.2.2.3 Effect of ferric iron's existing form

Literature showed that under irradiation of UV light, ferric iron would form from ferrous iron, so the objective of this experiment was to measure the effect of ferric iron on the decomposition of selenocyanate. Batch experiments were conducted with 0.0127 mmol/L selenocyanate (1 mg/L as Se) and 0.127 mmol/L ferric iron with no UV irradiation. Two pH conditions (pH 4, 10) were investigated, because a previous experiment found the ferric iron solution to be clear at pH 4, but to become brown immediately at pH 10. Also, it was observed that the selenium removals were different at the two pH values. These experiments were conducted to see the effect of these two conditions on the removal of selenium from the solution.

3.2.3 Sampling

All steps in sampling were conducted inside the anaerobic chamber to make sure that ferrous iron in solution were not oxidized by oxygen after sampling. The samples were taken at 6 to 10 different times with a 10 mL syringe, the sampling times were chosen based on the expected reaction rate. After collection, the samples were filtered

with 0.2- μm filter paper (Whatman). This is because we expected that insoluble elemental selenium would be generated by decomposition of selenocyanate. Also, we expected that ferric hydroxide solids would be formed in the experiments at high pH when ferrous iron was photo-oxidized by UV light and that those solids could potentially adsorb selenocyanate from solution. After filtration, the filtrate was prepared for analysis. A 1-ml portion of the filtrate was added to 9 mL of a solution containing 1% (V:V) concentrated nitric acid and 89% (V:V) deoxygenated deionized water contained in 15-mL centrifugal tube covered by aluminum foil. If the selenium sample could not be analyzed immediately, the centrifugal tube would be stored in a refrigerator at 4 °C.

3.3 Analytical procedures

3.3.1 Qualitative analysis

The Spectronic Holios Gamma UV-Vis Spectrophotometer (Thermo scientific) was used for qualitative analysis of selenocyanate. A 3-ml portion of the filtrate was transferred to a quartz cell with 1-cm path length. Then the cell was settled inside the spectrophotometer. The absorption spectra of selenocyanate were measured from 190 to 1000 nm. A broad peak was identified for selenocyanate between 190 and 300 nm.

3.3.2 Quantitative analysis

Samples that had been prepared as previously described were analyzed by Inductively Coupled Plasma-Mass Spectrometry (Perkin Elmer, NexIon 300D) (Figure 3.1). ICP-MS was used to analyze the soluble selenium concentration in the samples. The term “soluble” will be used, although it is recognized that small selenium solids that

pass through the filter would be included in the analysis. The instrumental operating conditions and data acquisition parameters are shown in Table 3.1.

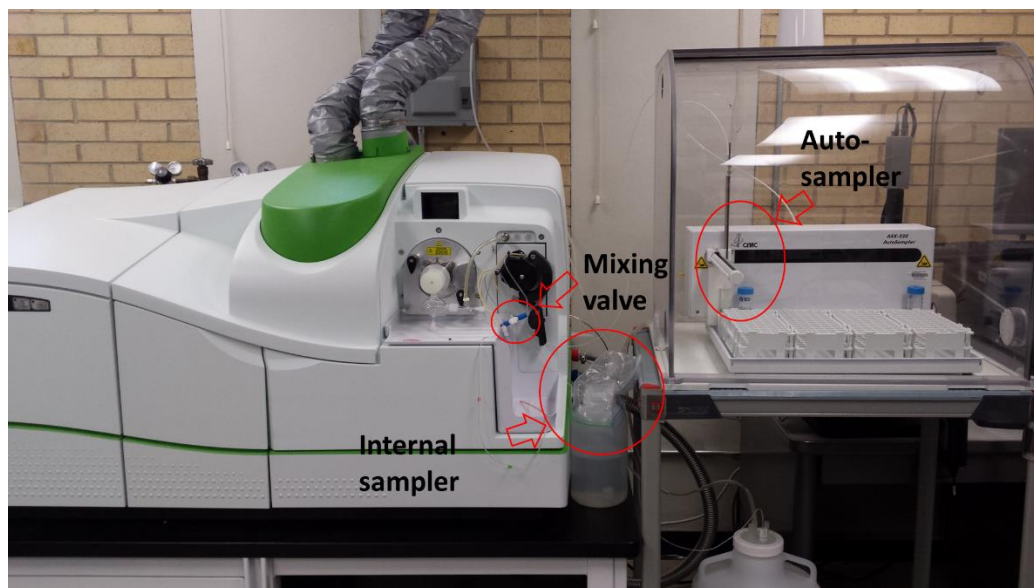


Figure 3.1 ICP-MS system

The auto-sampler takes the solution from the sample contained in a 15-mL centrifugal tube, while the internal sampler takes a sample of the internal standard. Then, the experimental sample and the internal standard are mixed (Figure 3.2), and the mixed solution is ready for analysis. The internal standards contains 5 ppb Ga in a solution of 3 % (v:v) methanol. The methanol is added to eliminate the effect of carbon ions in the sample. The standard curve was based on the normalized intensity (selenium intensity/gallium intensity).

Mass spectrometer	PerkinElmer ICPMS (NexION 300D)
RF Power	1600w
Deflector Voltage	-11.99v
Analyzer Mode	Standard
Plasma condition:	
Nebulizer Gas flow	1.0L/min
Plasma Gas Flow	17.5L/min
Auxiliary Gas Flow	1.1L/min
Nebulizer back pressure	53.1 psi
Measuring parameters:	
Sweeps/Reading	20
Readings/Replicate	1
Replicates	3
Internal standard	⁷¹ Ga in 3% (v:v) methanol
Measured isotope	⁷⁸ Se

Table 3.1 Instrumental operating conditions and data acquisition parameters

The ICP-MS was turned on for 30 minutes to warm up and then a daily performance check was conducted before the analysis. The standards were prepared at concentrations of 5, 10, 25, 50, 100 $\mu\text{g/L}$ and these solutions were used to develop a calibration curve every time samples were analyzed. One example of a standard curve is shown in Figure 3.3.

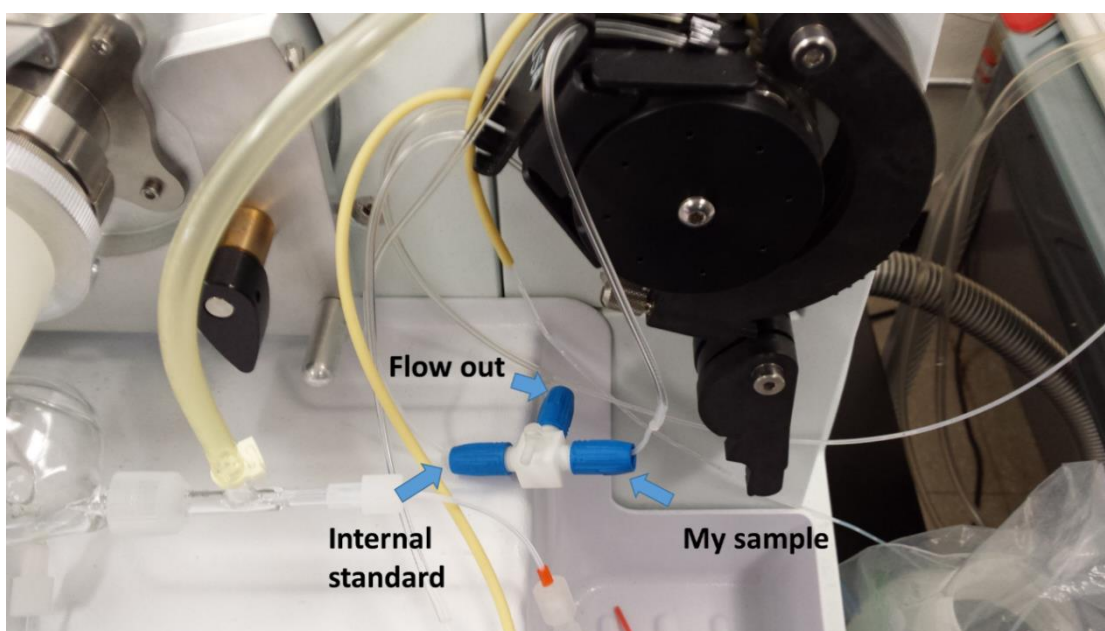


Figure 3.2 Valve system

Separate standard solutions were prepared using selenocyanate and selenite and used to make standard curves. Seven replicates of a selenocyanate solution of 20 $\mu\text{g/L}$ as Se were analyzed using each standard curve. The selenite curve showed an average of 20.80 $\mu\text{g/L}$ with S.D. of 0.86 $\mu\text{g/L}$ and the selenocyanate curve showed an average of 20.45 $\mu\text{g/L}$ with S.D. of 1.11 $\mu\text{g/L}$.

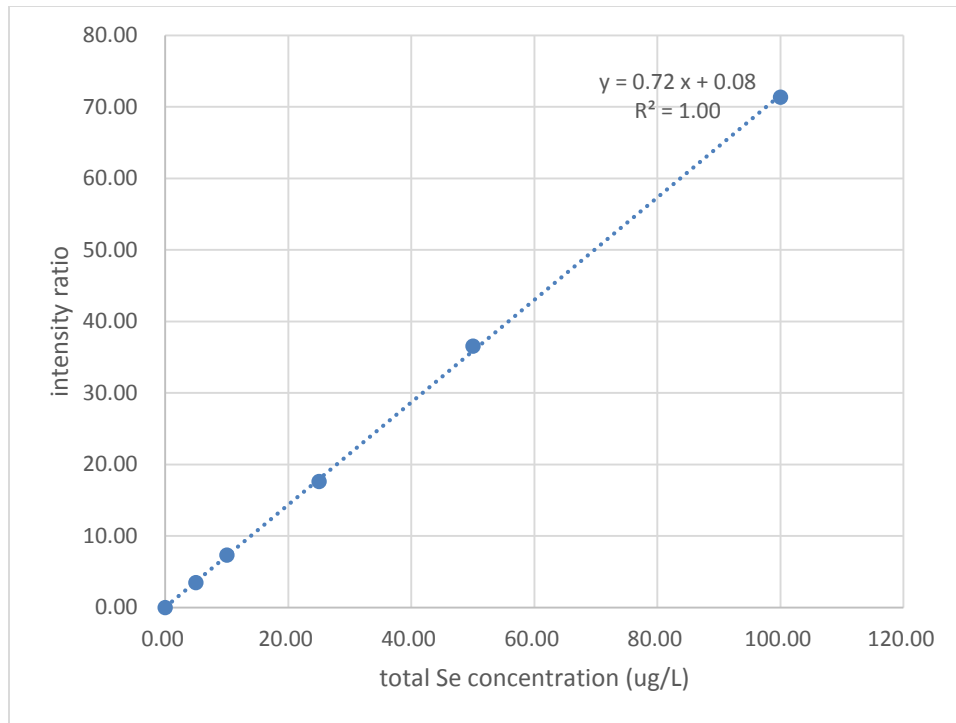


Figure 3.3 Example standard curve

The Method detection limit of this ICP-MS was calculated based on the 40 Code of Federal Regulations Part 136, Appendix B (USEPA, 2003) and Analytical Detection Limit Guidance (Wisconsin Department of Natural resources, 1996).

$$\text{MDL} = (\text{standard deviation}) \times (t - \text{value})$$

Data to do this calculation was obtained by preparing a selenocyanate solution with a selenocyanate concentration of 2.50 $\mu\text{g/L}$, which was chosen as the estimated MDL (0.50 $\mu\text{g/L}$) times 5. Seven samples of this solution were analyzed by ICP-MS and the results are shown in Table 3.2.

Sample	Measured conc. (µg/L)	% Recovery
1	2.48	99%
2	2.28	91%
3	2.29	92%
4	2.15	86%
5	2.14	86%
6	2.22	89%
7	2.11	84%
mean	2.24	90%
S.D.	0.13	

Table 3.2 Method detection limit data

The t-value with 6 degree of freedom is 3.143 so the MDL was calculated as 0.40 µg/L. The calculated MDL should meet the the following inequalities to be appropriate and it does.

$$\text{Calculated MDL} < \text{Spike Level} < 10 \times \text{Calculated MDL}$$

In summary, he analysis procedure for selenocyanate was shown to have a method detection limits of 0.4 µg/L; a total recovery of 90 % and a standard deviation of 0.13 µg/L.

4. RESULTS AND DISCUSSION

This section describes and explains results of all the experiments that were conducted in this research. There were two variables considered to affect the degradation kinetic experiments that were investigated -- pH and light irradiance. Before each variable was investigated, some control experiments were done to determine the base line for these sets of experiments.

4.1 Experiments of effect on pH

The research hypothesized that pH had a major effect on selenocyanate removal in the system under study. On one hand, pH may affect selenocyanate hydrolysis. At low pH, the selenocyanate molecule will break up and form insoluble elemental selenium, which directly decreases the soluble selenium concentration. On the other hand, pH may also have some effect on reactions of ferrous iron with UV light. Ferrous iron can photolyze to form ferric iron and the aqueous electron. Ferric iron is relatively insoluble and forms ferric hydroxide solids, which could adsorb selenium from solution and this would cause the concentration of soluble selenium to change. This set of experiments was conducted to investigate the decomposition of selenocyanate in the presence of UV light (254 nm) and ferrous iron at different pH values. In this set of experiments, the pH values were set to be 4, 7 and 10.

4.1.1 Blank control

The selenocyanate solution was added to a quartz cell and the cell was then kept in a dark environment. No reductant (Ferrous iron) was added and no UV light was

applied in these experiments. The pH values of the solutions were set at 4, 7 and 10. At each pH value, the concentrations of soluble selenium in solution at different times were analyzed by ICP-MS and the results are shown in Figures 4.1-4.3 (note different time scales). The results represent total soluble concentrations, because they were conducted by ICP-MS, which measures all selenium forms and they were conducted on samples after filtration removed solids. Because some insoluble selenium might pass the filter, it is possible that the analysis include some selenium present as small particles.

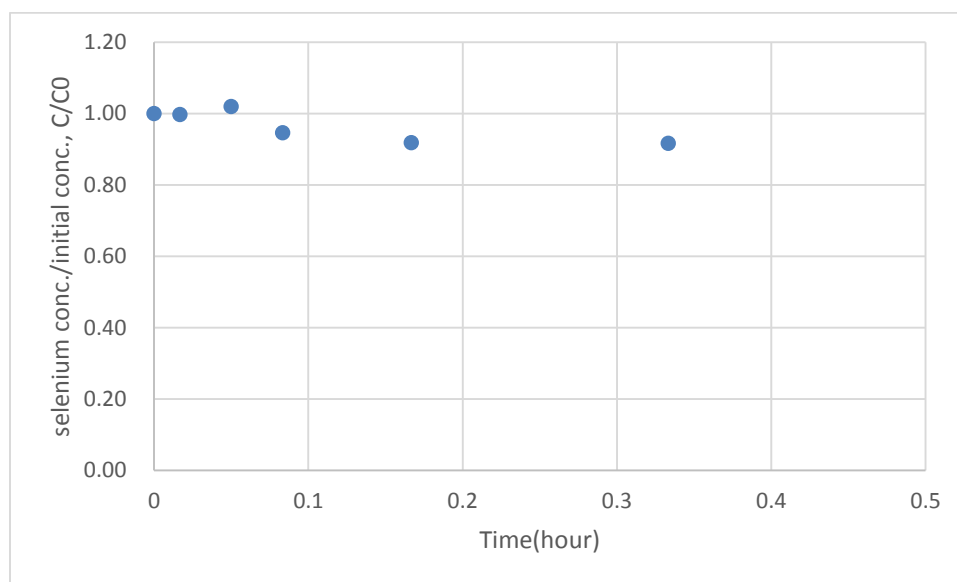


Figure 4.1 Soluble selenium concentrations over time at pH = 4 (blank control, initial selenocyanate as selenium = 0.71 mg/L)

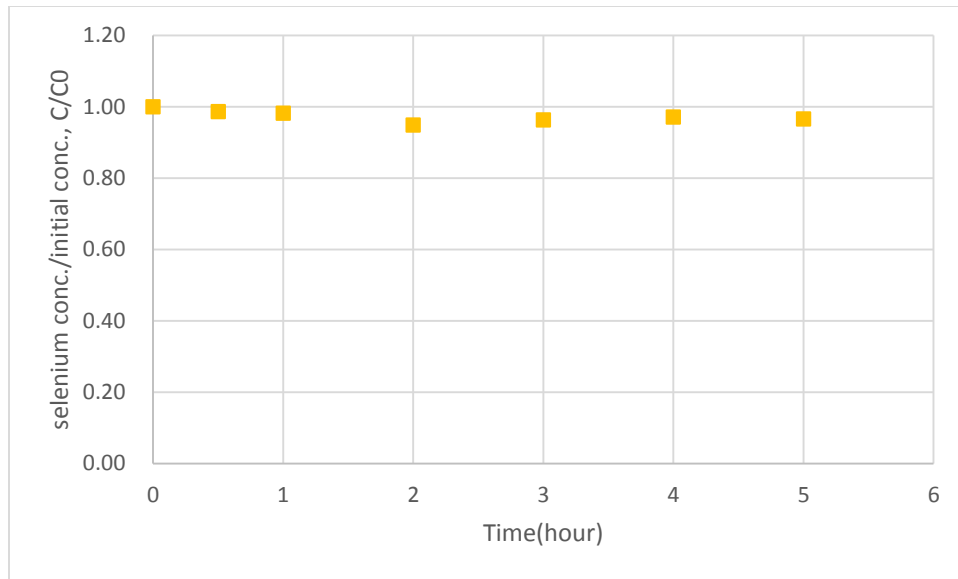


Figure 4.2 Soluble selenium concentrations over time at pH = 7 (blank control, initial selenocyanate as selenium = 0.95 mg/L)

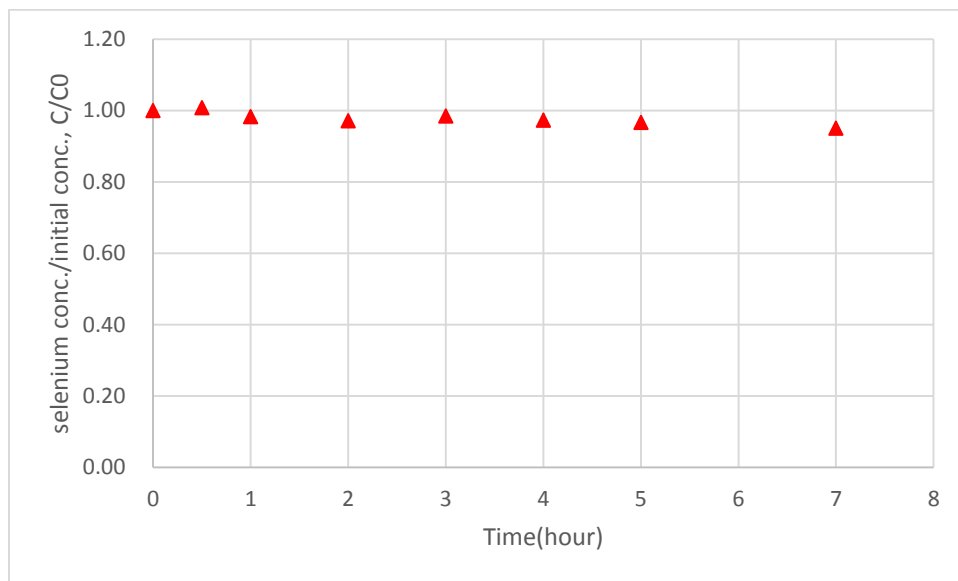


Figure 4.3 Soluble selenium concentrations over time at pH = 10 (blank control, initial selenocyanate as selenium = 0.98 mg/L)

These figures show that the soluble selenium concentration decreased fastest at pH 4, although only 10% of the initial selenium in selenocyanate was converted to elemental selenium in 0.3 hours. However, when pH increased to 7 and 10, the selenium was relatively stable and it did not change more than 5% in 7 hours. This was consistent with Golub and Skopenko's (1965) statement. They pointed out that when a selenocyanate solution was alkaline, it was stable, but it started to decompose when pH was reduced to 5.

4.1.2 Reagent control

The reagent control experiments were conducted to measure the loss of selenium due to any reaction with ferrous iron without UV light. These experiments used a 10 mg/L concentration of ferrous iron, which was about 10 times the selenium concentration. The pH was also set at 4, 7 and 10. Figures 4.4-4.6 show the soluble selenium concentrations over time at three pH values.

The reagent control experiments showed behavior that was very similar to that seen in the blank control experiments. At pH 4, the reduction in selenium concentration was relatively fast and it decreased 10% in 20 minutes. However, selenium concentration was stable at pH 7 and 10 even after 5 or 7 hours. These observations mean that the effect of ferrous iron was insignificant.

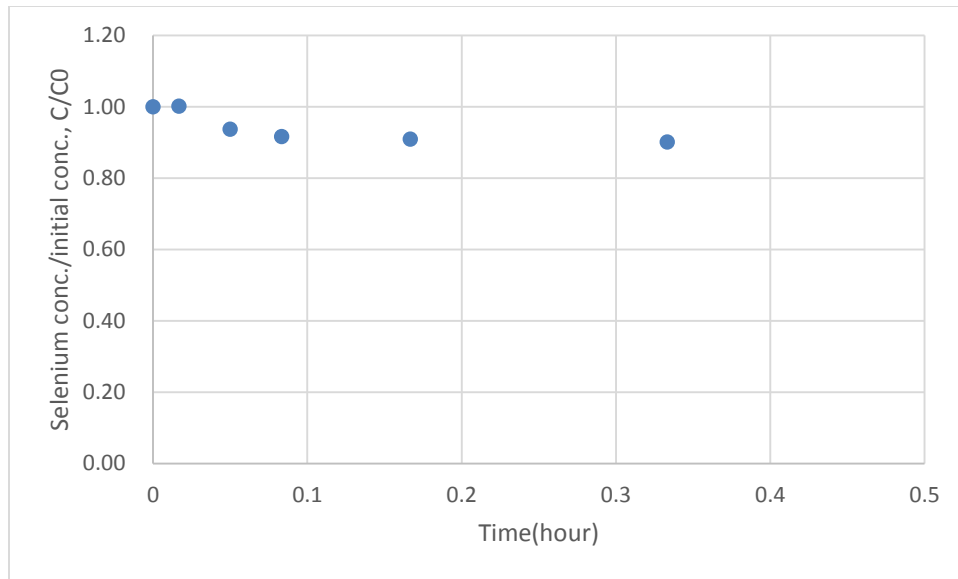


Figure 4.4 Soluble selenium concentrations over time at pH = 4 (reagent control, ferrous iron = 10 mg/L, initial selenocyanate as selenium = 0.69 mg/L)

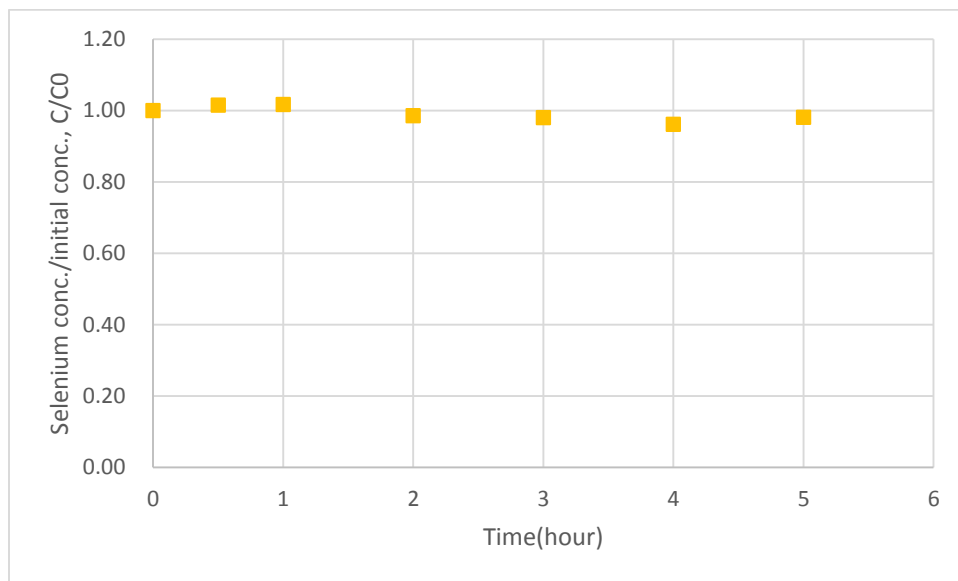


Figure 4.5 Soluble selenium concentrations over time at pH = 7 (reagent control, ferrous iron = 10 mg/L, initial selenocyanate as selenium = 0.78 mg/L)

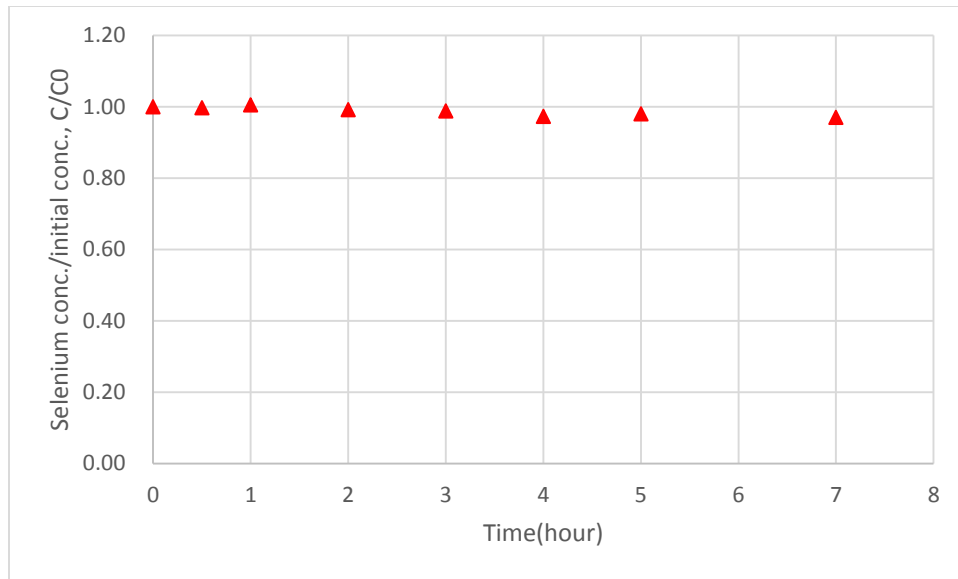


Figure 4.6 Soluble selenium concentrations over time at pH = 10 (reagent control, ferrous iron = 10 mg/L, initial selenocyanate as selenium = 0.99 mg/L)

4.1.3 Light control

The light control experiment was conducted with UV light (254 nm) at 5000 $\mu\text{W}/\text{cm}^2$ without ferrous iron. At pH 4, the selenocyanate decomposition is shown in Figure 4.7.

Figure 4.7 indicates that selenium concentration decreases sharply in first 0.02 hour, and then this decline slows down and the concentration becomes stable after about 0.07 hour. Figures 4.8 and Figure 4.9 show the selenium concentrations at pH 7 and 10. They both show the same trend that was shown in Figure 4.7, but with changes occurring over a longer time range.

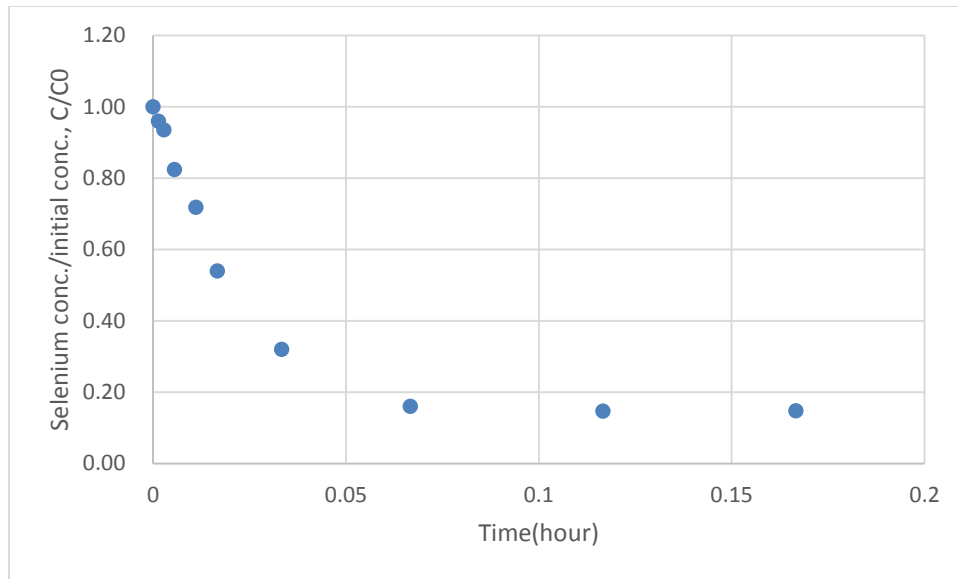


Figure 4.7 Soluble selenium concentrations over time at pH = 4 (light control, UV irradiance = 5000 $\mu\text{W}/\text{cm}^2$, initial selenocyanate as selenium = 0.98 mg/L)

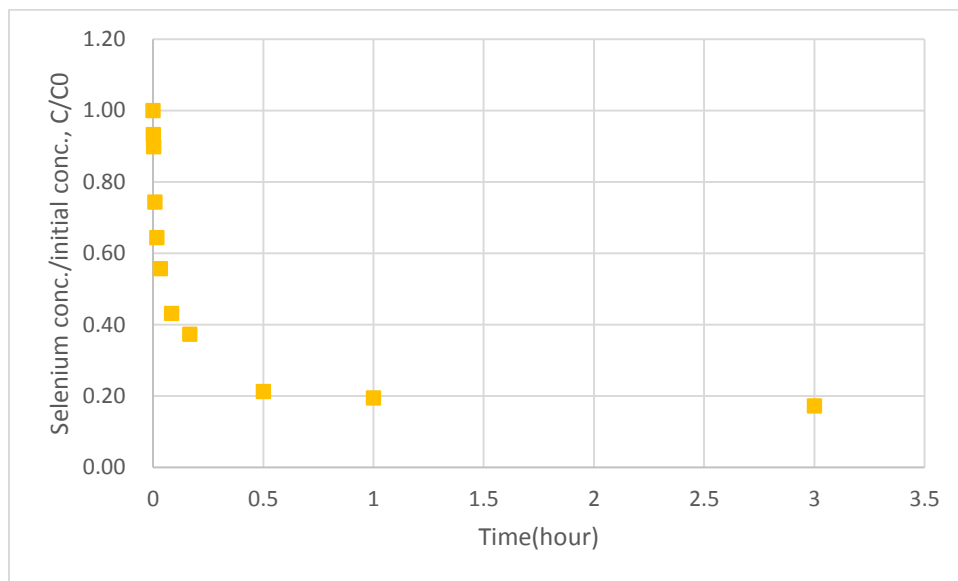


Figure 4.8 Soluble selenium concentrations over time at pH = 7 (light control, UV irradiance = 5000 $\mu\text{W}/\text{cm}^2$, initial selenocyanate as selenium = 0.97 mg/L)

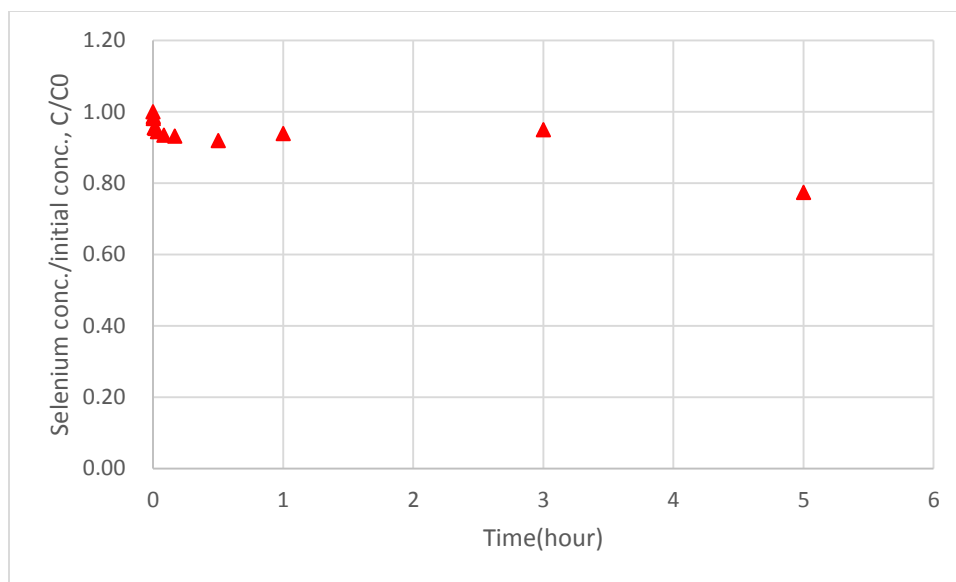


Figure 4.9 Soluble selenium concentrations over time at pH = 10 (light control, UV irradiance = 5000 $\mu\text{W}/\text{cm}^2$, initial selenocyanate as selenium = 0.99 mg/L)

The sharp decrease in selenium concentration at the beginning of the experiments was found through all pH values, as shown in Figures 4.7 to 4.9. This may be caused by the direct photolysis of selenocyanate by UV irradiation. Dogliotti and Hayon (1968) observed that the thiocyanate would absorb UV light and then decompose into elemental sulfur. Considering that sulfur and selenium are in the same column in the Periodic Table, selenocyanate may also absorb UV light, which might lead to the photolysis of selenocyanate. The ability of selenocyanate to absorb UV light at 254 nm was confirmed by measurements of the absorption of a selenocyanate solution with selenium concentration of 20 mg/l over the wavelength range from 190 nm to 1000 nm (Figure 4.10).

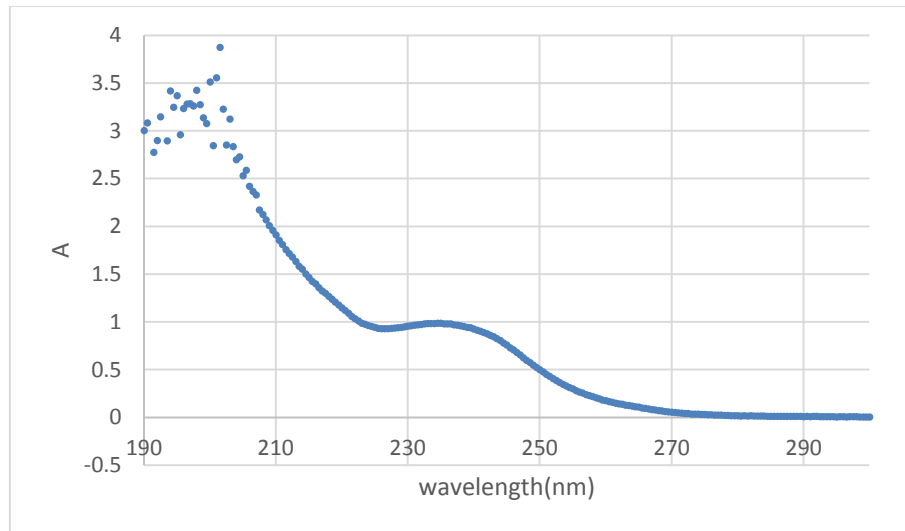
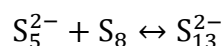
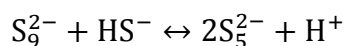


Figure 4.10 UV Light Absorption of Selenocyanate solution

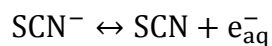
After the fast degradation at the beginning, the selenium concentration decline rate became much slower, even negligible. The mechanism of this selenium concentration plateau is not clear, but one possible hypothesis to explain this may be the inner filter effect of selenium and a fast back reaction. Luria and Treinin (1968) proposed that these mechanisms were responsible for the thiocyanate degradation rate decrease. The inner filter effect of selenium means that the generated elemental selenium may reflect or scatter the UV light that otherwise would go through the solution and be absorbed by selenocyanate. The back reaction would be the regeneration of selenocyanate from elemental selenium and cyanide. Another hypothesis is that incomplete removal of elemental selenium particles by filtration causes the concentration plateau. Some of the elemental selenium particles that were generated could have had smaller diameters than the pore size of the filters (0.2- μm), thus some

smaller selenium particles could stay in the samples after filtration. However, the incomplete filtration alone is less likely to explain the plateau in total selenium, because with longer time of irradiation by UV light, the small elemental selenium particles would have more time to grow into particles that are large enough to be filtered out. If particle growth occurs without nucleation of small particles, then the final measured soluble selenium concentrations should continue to decrease. However, this mechanism could be a partial explanation of the observed behavior, along with other theories, such as the polyselenide theory, which is described below.

Another hypothesis to explain this may be the generation of polyselenide. Kleinjan et al. (2005) investigated the kinetics of polysulfide formation and proposed the possible mechanism shown below:



The formation of polysulfide requires the coexistence of elemental sulfur and sulfide. When thiocyanate was under irradiation by UV light, Luria and Treinin (1968) observed the formation of elemental sulfur. At the same time, Dogliotti and Hayon (1968) claimed another reaction path of thiocyanate under UV irradiation.



The generated electron is a highly reactive reductant and has the potential to react with elemental sulfur to produce sulfide. Also, Dogliotti and Hayon (1968) observed a

strong smell of H_2S , indicating the formation of sulfide. As a result, there is the possibility that polysulfide forms when thiocyanate is irradiated by UV light.

As selenium and sulfur are in the same column in the Periodic Table, they share some similar chemical properties. Also, selenocyanate is isomorphous with thiocyanate, so selenocyanate may follow the same process of photolysis as thiocyanate. Under the irradiation of UV light, selenocyanate may decompose to elemental selenium and selenide, which may later react with each other and generate polyselenide.

Another experiment was conducted to demonstrate the mechanism of selenocyanate photolysis over time. Figure 4.11 shows the selenocyanate absorbance after irradiation at different times up to 1 hour at pH 7. Figure 4.11 shows that the selenocyanate concentration decreases over time as photolysis occurs. However, Figure 4.8 shows that the total selenium concentration is already stable between half an hour and an hour.

Summing up these two results, selenocyanate concentration measured by UV absorbance is decreasing, but total selenium concentration stays the same. This indicates that photolysis of selenocyanate occurs during the whole time of UV light irradiation and so does formation of elemental selenium. However, the soluble selenium concentration does not keep decreasing, but becomes stable after a certain time, which means that the elemental selenium formed by photolysis of selenocyanate is likely being converted to another soluble form of selenium. This is consistent with the hypothesis of polyselenide generation.

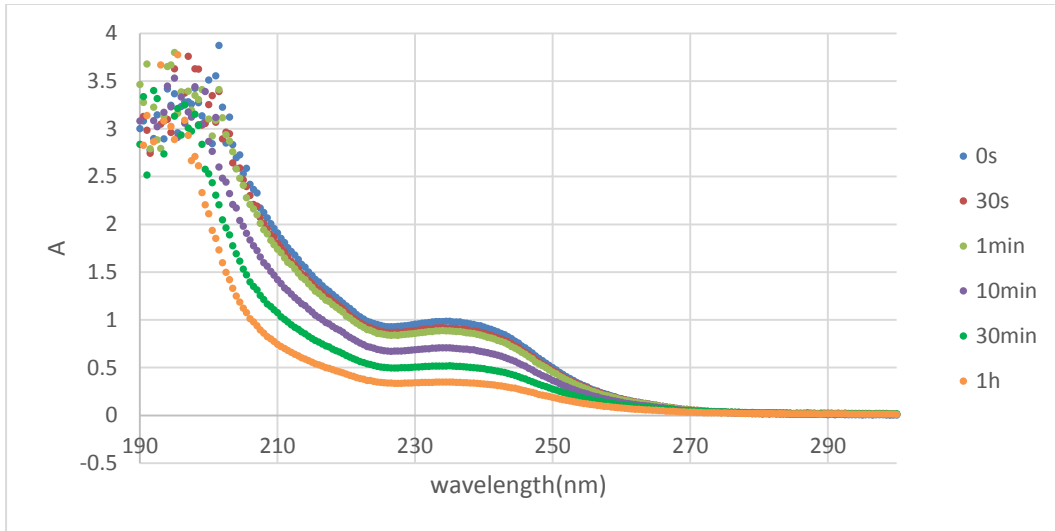


Figure 4.11 UV light absorbance of selenocyanate solution over time at pH = 7 (UV irradiance = $5000 \mu\text{W}/\text{cm}^2$)

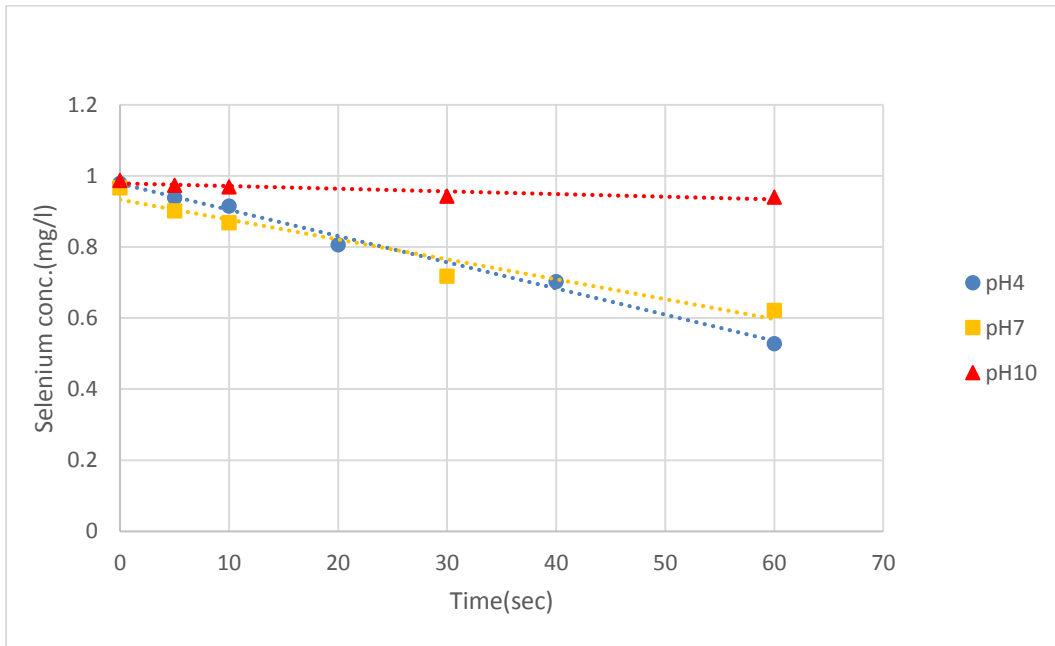
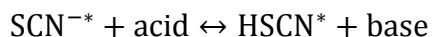
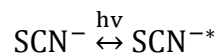


Figure 4.12 Soluble selenium concentrations at three pH values during the first minute of irradiation (light control, UV irradiance = $5000 \mu\text{W}/\text{cm}^2$)

	Initial Rate (mg·L ⁻¹ ·s ⁻¹)
pH 4	0.0074
pH 7	0.0056
pH 10	0.0007

Table 4.1 Initial reaction rates at different pH values (UV irradiance = 5000 μW/cm²)

The kinetics of this control experiment was examined by calculating initial rates using data for the first minute (Figure 4.12) and the results are listed in Table 4.1. These results show that pH has a pronounced effect on selenocyanate photolysis. The fastest selenocyanate decomposition rate occurred at pH 4, and as pH increased, the initial rate decreased. Luria and Treinin (1968) observed the same pH dependence trend for thiocyanate photolysis. They suggested a mechanism from their results:



The superscript “*” means an excited state. They stated that the primary quantum yield of HSCN* was higher than that of SCN^{-*}, indicating that HSCN* is more efficient in utilizing photons for dissociation than SCN^{-*}. Since HSCN* would predominate at lower pH this explains how lower pH could improve the rate of thiocyanate photolysis. Again, as selenocyanate is isomorphous with thiocyanate, maybe the same mechanism causes selenocyanate photolysis to be faster at acid pH.

4.1.4 ARP experiments (ferrous iron + UV light)

A series of experiments was conducted to investigate the effect of pH on selenocyanate decomposition with the ferrous iron/ultraviolet light advanced reduction process (Fe/UV-ARP). Under UV light irradiation, the weak Se-C bond from selenocyanate would break to produce elemental selenium. Meanwhile, the aqueous electron could be produced when ferrous iron is under irradiation and this aqueous electron may be able to degrade selenocyanate to elemental selenium. At the same time, the ferric iron that is formed may also react with selenocyanate directly or form ferric hydroxides to adsorb selenocyanate. Figure 4.13 shows the results of ARP experiments at three pH values. They all show the same trend that was observed in the light control experiment: selenium concentration decreased fast at the beginning and then became stable for a long time. In the first 0.05 hour, the degradation rate was greatest at pH 4, followed by the rate at pH 7 and the degradation rate at pH 10 was the slowest. However, it is interesting that the selenium concentration became stable after about 0.1 hour, which was almost the same time as the selenium concentration became stable in the light control experiments. In the plateau period, the selenium concentration at pH 7 was lower than that at pH 4. One possibility for this is that at pH 4, the most of the iron that is present (ferrous iron added and ferric iron generated by photolysis) would exist in solution as Fe^{2+} , Fe^{3+} and soluble ferric hydroxides. Soluble ferrous iron was shown to be inert with selenocyanate. However, when pH increases to 7, a large part of ferric iron forms solid phases such as $\gamma\text{-FeOOH}$ or amorphous ferric hydroxides. These solid phases could adsorb selenium from the solution, thereby decreasing the soluble selenium

concentration in the solution. Anbar and Holland (1992) confirmed that large amounts of ferric precipitates are generated at pH 7 in their study. At pH 10, although the ferric hydroxide solids that are formed might help the removal of selenium that is present in the form of products of selenocyanate photolysis, but this reaction was too slow, so the overall selenium removal does not show much improvement in the presence of iron.

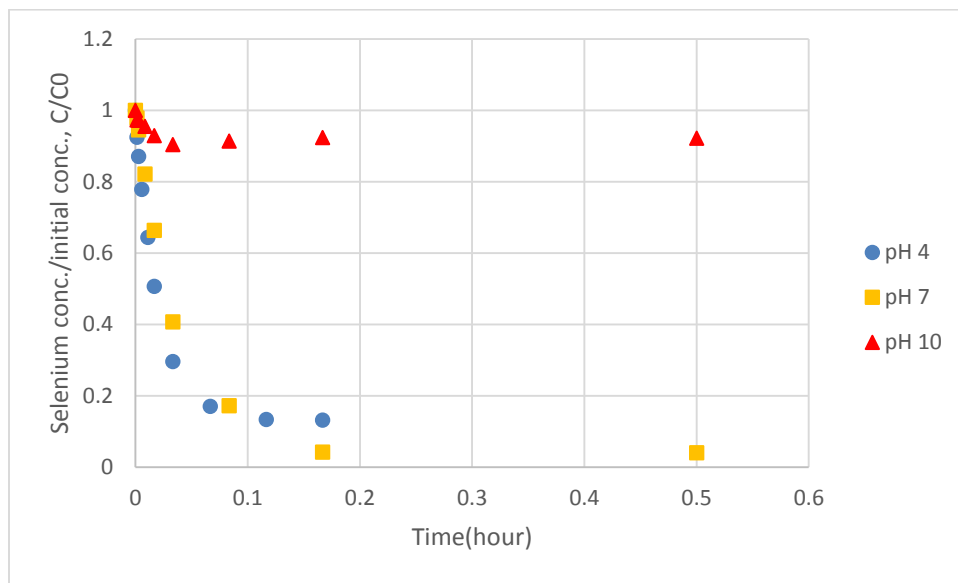


Figure 4.13 Soluble selenium concentrations change over time at 3 pH values with Fe/UV-ARP (ferrous iron = 10 mg/L, UV irradiance = 5000 $\mu\text{W}/\text{cm}^2$, initial selenocyanate as selenium = 1 mg/L)

The initial rates were calculated for the Fe/UV-ARP experiments using data for the first minutes (Figure 4.14), and the values are shown in Table 4.2 along with the rates for the light control experiments for comparison.

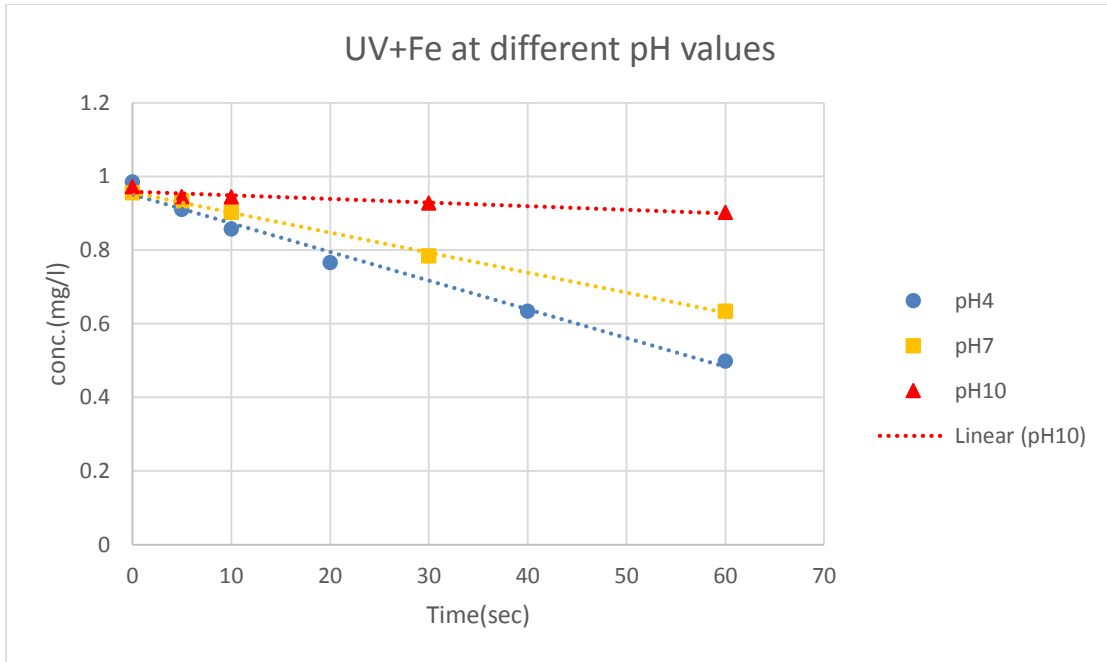


Figure 4.14 Soluble selenium concentrations at three pH values in first minute for the Fe/UV-ARP (ferrous iron = 10 mg/L, UV irradiance = 5000 $\mu\text{W}/\text{cm}^2$)

	Initial Rates ($\text{mg}\cdot\text{L}^{-1}\text{s}^{-1}$)	
	UV Only	Fe/UV-ARP
pH 4	0.0074	0.0078
pH 7	0.0056	0.0054
pH 10	0.0007	0.0010

Table 4.2 Initial reaction rates at different pH values for UV irradiation (UV irradiance = 5000 $\mu\text{W}/\text{cm}^2$) and Fe/UV-ARP (ferrous iron = 10 mg/L, UV irradiance = 5000 $\mu\text{W}/\text{cm}^2$)

Table 4.2 shows that the initial rate does not change much in ARP experiments, which means that the effect of ferrous iron is insignificant in this set of ARP experiments.

Next, experiments were conducted with UV and the UV-Fe ARP over longer periods of time at each pH value. Figure 4.15-4.17 presents the results. These figures show that the data for the ARP (UV-Fe) and the light control (UV) basically share the same trend at the three pH values: a fast decrease in soluble selenium concentration at first and then the concentration becomes stable at later times.

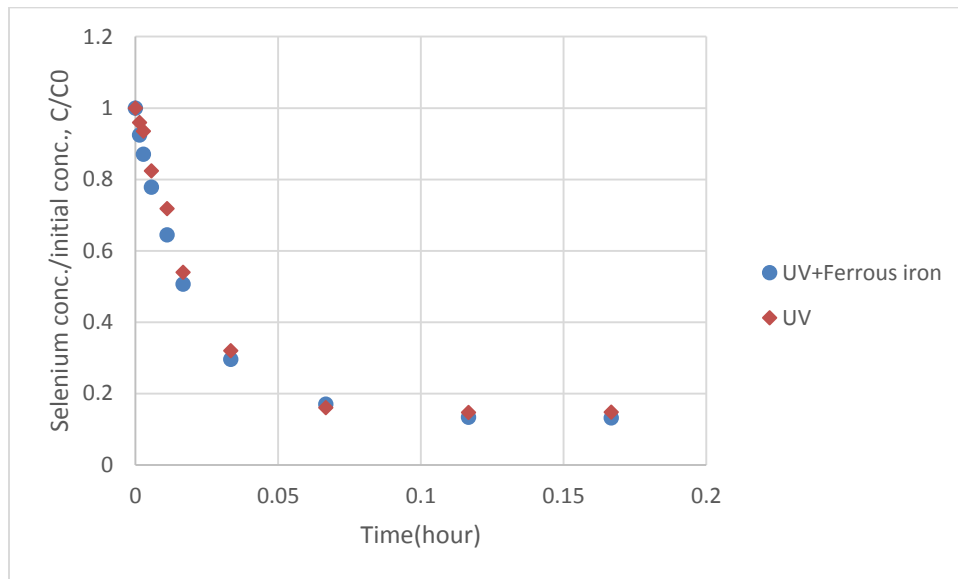
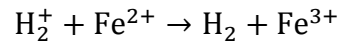
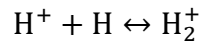
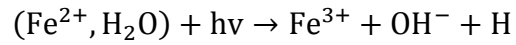


Figure 4.15 Soluble selenium concentrations over time at pH = 4 (UV-Fe ARP and UV alone)

Figure 4.15 shows that at pH 4, results for the two experiments are almost the same. The reason may be that at low pH values, ferrous iron would react in the present

of UV light to form hydrogen atoms, rather than aqueous electrons. The hydrogen atoms ultimately form hydrogen gas as proposed by Hayon and Weiss (1960).



Because the aqueous electron was not available for the decomposition of selenocyanate, the presence of Fe^{2+} did not have an effect on conversion of selenocyanate to elemental selenium.

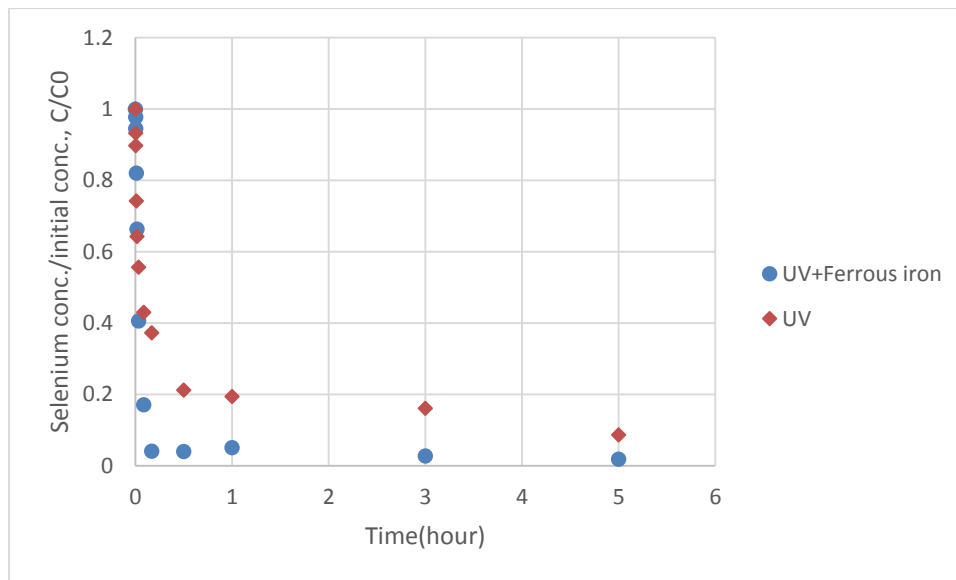


Figure 4.16 Soluble selenium concentrations over time at pH = 7 (UV-Fe ARP and UV alone)

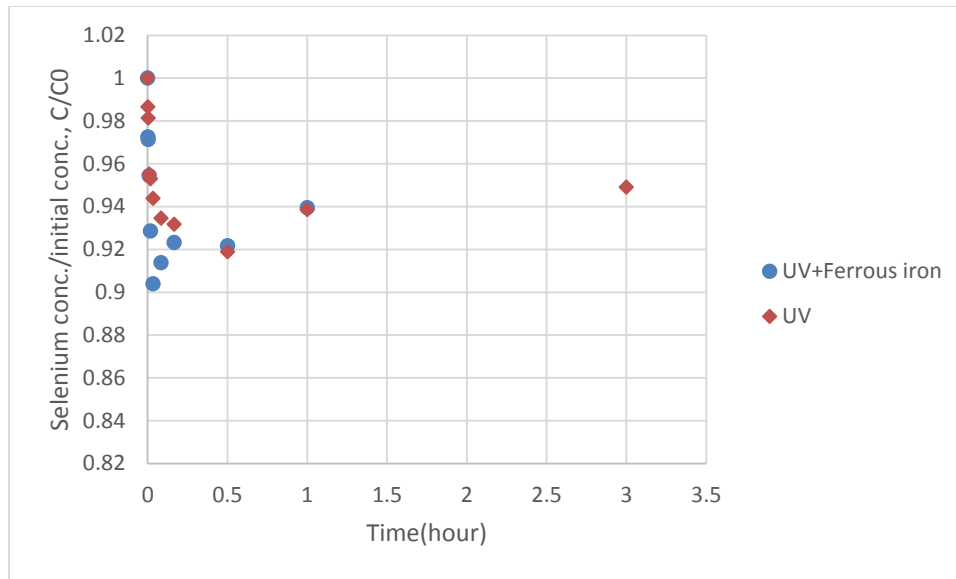


Figure 4.17 Soluble selenium concentrations over time at pH = 10 (UV-Fe ARP and UV alone)

Figures 4.16 and 4.17 show that the declines in selenium concentration were fast at early times for both the light control (UV) and ARP experiments (UV/Fe) at pH 7 and 10. However, the experiments with ferrous iron at pH 7 shows better selenium removals at the later times. Ferrous iron does not play an important role in the first, fast removal stage, because at neutral to high pH values, the reaction mixture may exist as suspensions containing $\text{Fe}(\text{OH})_2(\text{s})$ and the UV light at 254 nm may not be absorbed by those solids. Schrauzer and Guth (1976) found that at pH from 8 to 10, the flocculated $\text{Fe}(\text{OH})_2(\text{s})$ was responsible for the hydrogen generation in the dark. The rate of H_2 production from $\text{Fe}(\text{OH})_2$ was accelerated with UV irradiation, and wavelengths from 300 to 330 nm was the most effective. Borowska and Mauzerall (1986) investigated the formation of hydrogen with UV light and ferrous iron solution. They found that

hydrogen gas forms at low pH values with UV light of wavelength less than 300 nm and the species responsible for the photochemical reaction was aqueous Fe^{2+} . However, when the UV light had a wavelength of 300 nm or higher, flocculated $\text{Fe}(\text{OH})_2(\text{s})$ might also be responsible for the hydrogen gas formation at higher pH values (6 or higher). Their conclusions may be consistent with the present study: at pH 4, aqueous Fe^{2+} was the reactive species but was consumed by hydrogen generation. At pH 7 or pH 10, the suspended $\text{Fe}(\text{OH})_2(\text{s})$ was the reactive species; however, it was unable to absorb UV light at 254 nm. Probably these are the reasons that ferrous iron could not improve the selenocyanate reaction rate during irradiation with 254 nm UV light

However, experiments with ferrous iron show better selenium removal than those without ferrous iron, at the end of the experiment. As indicated before, this better removal might be the result of selenium compounds adsorbing onto ferric hydroxide solids. Anbar and Holland (1992) observed that at pH 7, Fe^{2+} dissolved in solution mixed with Mn^{2+} were rapidly oxidized to Fe^{3+} under UV irradiation (180 -1400 nm) in an oxygen free environment, and the Fe^{3+} precipitated as $\gamma\text{-FeOOH}$ or as amorphous ferric hydroxide solids. The precipitated ferric hydroxide is an ideal adsorbent and may be responsible for the better removal of selenium.

4.2 Experiments of effect on light irradiance

UV light has a big effect on selenocyanate removal in these systems because it promotes selenocyanate hydrolysis directly. This set of experiments was conducted to investigate the decomposition of selenocyanate in the presence of UV light (254nm) at different values of light irradiance.

This set of experiment was conducted at a fixed pH (pH 7) without ferrous iron, because the presence of ferrous iron did not improve the selenium removal in the fast decomposition stage in previous experiments. Also, experiments without ferrous iron would be simpler to conduct and the results would be easier to interpret.

In this set of experiments, light irradiance was set at 3000, 5000 and 7000 $\mu\text{W}/\text{cm}^2$. Figure 4.18 compares the soluble selenium concentrations at three values of light irradiance over one hour. Soluble selenium concentrations follow the same trend that was discussed previously, i.e. fast decrease followed by a stable concentrations. Figure 4.19 shows the soluble selenium concentrations during the stage of fast decrease, which was observed during the first minute. The initial reaction rates were calculated and they are shown in Table 4.3. As the UV light is the only energy responsible for the selenocyanate photolysis, it is reasonable that the initial reaction rate is greatest when light irradiance is 7000 $\mu\text{W}/\text{cm}^2$, followed by the rate at 5000 $\mu\text{W}/\text{cm}^2$, and finally the rate at 3000 $\mu\text{W}/\text{cm}^2$.

Figure 4.20 shows the relationship between initial reaction rates and light irradiance. It shows that initial rates for selenocyanate degradation are proportional to light irradiance. The linear regression gives an intercept of 0. This result is reasonable, because with no UV light, the selenocyanate hydrolysis at pH 7 is negligible. This behavior is also consistent with the fact that UV light is the only energy used in these experiments that could lead to the conversion of selenocyanate.

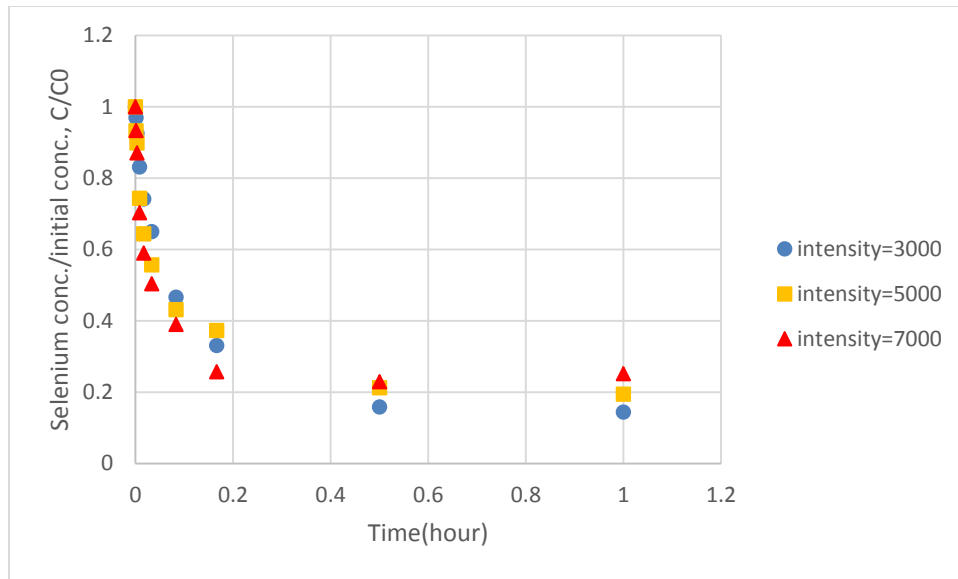


Figure 4.18 Soluble selenium concentrations over time at three values of light irradiance

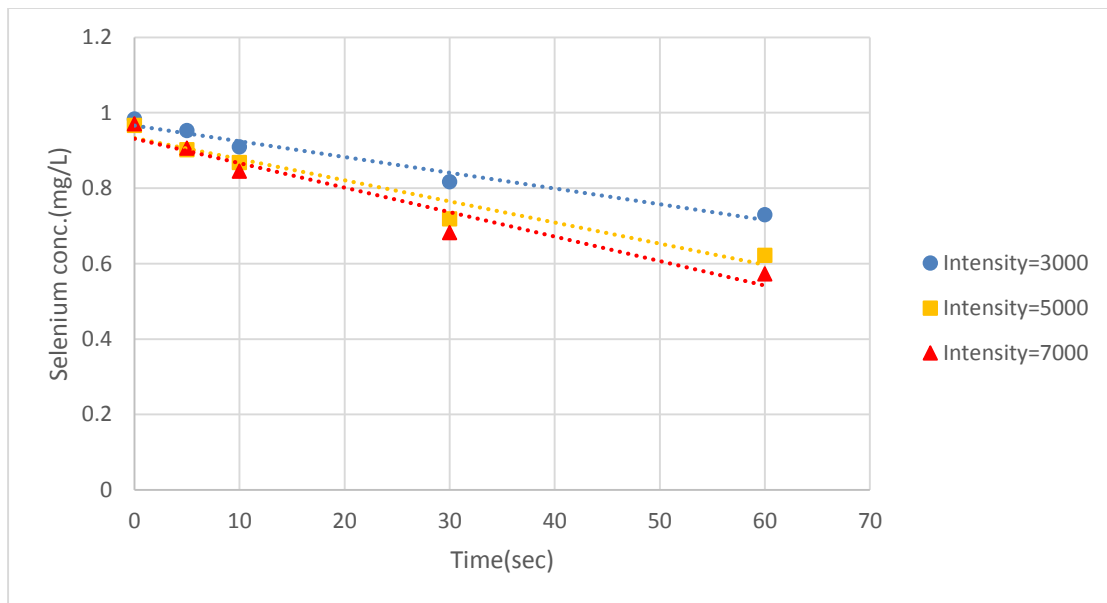
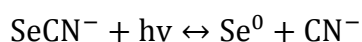


Figure 4.19 Soluble selenium concentrations during the first minute for three values of light irradiance

Irradiance of UV Light (254 nm)	Initial Reaction Rates (mg·L ⁻¹ ·s ⁻¹)
3000 μW/cm ²	0.0042
5000 μW/cm ²	0.0056
7000 μW/cm ²	0.0065

Table 4.3 Initial reaction rates at different values of light irradiance

The thiocyanate photolysis reaction was presented in Chapter 2 and it is expected that selenocyanate would have a similar photolysis process.



Crittenden et.al. (2012) related the average photolysis rate to the concentration of the compound being photolyzed and the average light irradiance.

$$r = \frac{\varphi \cdot I_{p0}}{b} \cdot (1 - \text{EXP}(-\varepsilon'(\lambda) \cdot C \cdot b))$$

Where r = average photolysis reaction rate, mol/cm³·s; φ = quantum yield at wavelength λ , mol/einstein; $\varepsilon'(\lambda)$ = base-e molar absorptivity of light-absorbing solute at wavelength λ , L/ mol·cm; C = concentration of light-absorbing solute, mol/L; I_{p0} = photonic intensity at wavelength λ that enters reactor, einstein/cm²·s; b = effective length of light path, cm; λ = wavelength, nm.

In this system, only a little light was absorbed, so the term $\varepsilon'(\lambda) \cdot C \cdot b$ is small. The exponential term $\text{EXP}(-\varepsilon'(\lambda) \cdot C \cdot b)$ can be expanded by Taylor expansion:

$$\text{EXP}(-\varepsilon'(\lambda) \cdot C \cdot b) = 1 - \varepsilon'(\lambda) \cdot C \cdot b + \frac{(\varepsilon'(\lambda) \cdot C \cdot b)^2}{2!} - \frac{(\varepsilon'(\lambda) \cdot C \cdot b)^3}{3!} + \dots$$

When $\varepsilon'(\lambda) \cdot C \cdot b$ is small, all terms after the second one can be ignored, so

$$EXP(-\varepsilon'(\lambda) \cdot C \cdot b) \approx 1 - \varepsilon'(\lambda) \cdot C \cdot b$$

$$\text{And, } r \approx \frac{\varphi \cdot I_{p_0}}{b} \cdot (1 - (1 - \varepsilon'(\lambda) \cdot C \cdot b)) = \varphi \cdot I_{p_0} \cdot \varepsilon'(\lambda) \cdot C$$

As Crittenden et al. (2012) state, the photolysis reaction rate is the product of the quantum yield (φ) and the rate of photon absorption, which for this experimental system is $I_{p_0} \cdot \varepsilon'(\lambda) \cdot C$. The quantum yield is dependent on the compound absorbing the light and the wavelength of light. The rate of photon absorption depends on incoming photonic intensity, and the absorptivity and concentration of the solute that absorbs light. This equation states that the initial photolysis reaction rate is proportional to the incoming photonic intensity, when absorbing solute absorptivity and absorbing solute concentration are constant. In this system, the absorbing solute absorptivity is constant and so is the initial absorbing solute concentration; therefore the initial photolysis reaction rate is predicted to be proportional to the incoming photonic intensity, which is proportional to the light irradiance. This is what was observed (Figure 4.20).

Interestingly, although the initial rate is proportional to light irradiance, Figure 4.18 shows the final selenium concentration at the stable stage has the opposite relationship with light irradiance. This may be caused by the generation of other soluble selenium forms such as polyselenide. More elemental selenium and selenide may be generated from selenocyanate photolysis at 7000 $\mu\text{W}/\text{cm}^2$ than that at 5000 and 3000 $\mu\text{W}/\text{cm}^2$ during the initial part of the experiment, which leads to more potential generation of polyselenide. Polyselenide may have the same properties as polysulfide, so it would be soluble in water. In fact, figure 4.18 shows that the soluble selenium concentration at the end of the experiment is higher at higher UV light irradiance. This

may be caused by elemental selenium being converted to polyselenide faster at higher irradiance. This would result in more of the polyselenide remaining in the solution after filtration, resulting in higher measured soluble selenium concentrations at the end of the experiment.

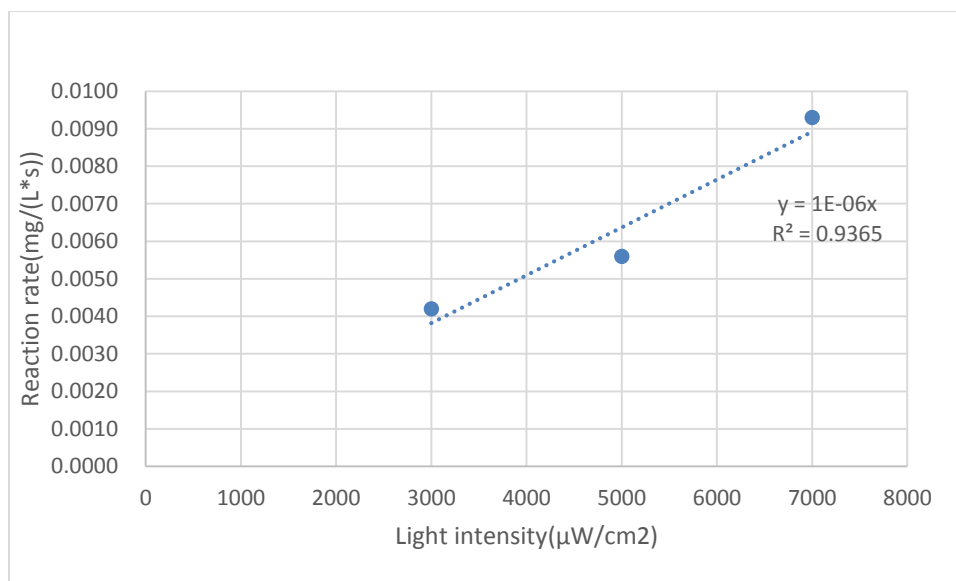


Figure 4.20 Effect of light irradiance on initial rates

4.3 Experiments of effect on ferric iron

Ferrous iron was not observed to improve the initial reaction rate of selenocyanate with UV light (Table 4.2); however, it could improve the selenium removal at end of the experiment. This has been explained as the result of adsorption of selenium by ferric hydroxide solids produced by photo-oxidation of ferrous iron. A set of experiments was conducted to investigate the effect of ferric iron at pH 4 and pH 10 on selenate decompositions without UV irradiation. The initial selenocyanate

concentration was 1 mg/L as Se, and the ferric iron concentration was 10 mg/L. Figure 4.21 shows the results of these experiments.

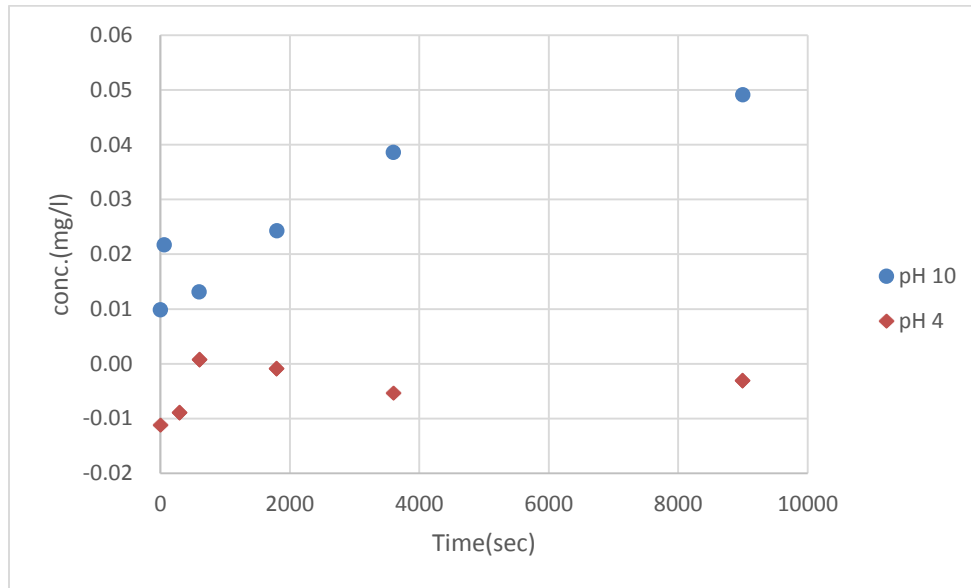


Figure 4.21 Soluble selenium concentrations over time at 2 pH values

Figure 4.21 indicates that at high pH, the presence of ferric iron results in greater loss of selenium from solution, which is consistent with results of previous experiments (Figure 4.15 and 4.16). This might indicate that the increased removal of selenium was due to adsorption onto ferric hydroxide solids. However, this is contradicted by the observations of Parida et al. (1995) and Balistrieri and Chao (1990). They found that selenium adsorption onto iron hydroxides increased with decreasing pH. The difference may be explained by the different selenium forms in solution. In their research, selenium was present as selenite; however, in the present research, selenocyanate was used and it may have been converted to other species such as polyselenides.

5. CONCLUSION

High levels of selenocyanate exist in some refinery and mining wastewaters generated from processing oil or minerals from seleniferous formations and they pose a great risk to humans and the environment. The goal of this study was to investigate the ability of an ARP that combines UV (activation method) and ferrous iron (reductant) to remove of selenocyanate from water. The conclusions of this research are listed below. They can be used to make the ARP methods more effective. Also, they indicate that a new method can be used to remove selenocyanate, which could supplement existing selenium control systems.

1. The blank control experiment indicates that some hydrolysis of selenocyanate occurs at low pH.
2. The reagent control experiment indicates that the ferrous iron alone will not improve selenocyanate removal.
3. The light control experiments indicate that photolysis is able to degrade selenocyanate. They show a sharp initial concentration decline, followed by stable soluble selenium concentrations. The initial rate of loss of soluble selenium increases as pH decreases.
4. The ARP experiments with ferrous iron and UV light showed that addition of iron did not improve the initial selenocyanate decomposition rate, however, addition of ferrous iron did decrease the final concentration of soluble selenium at high pH.

5. The light irradiance experiment indicates that the selenocyanate degradation rate is proportional to the light irradiance.

6. RECOMMENDATION

Results of this research indicate that the following future studies are needed.

1. Effects of different selenocyanate initial concentrations on removal of soluble selenium should be evaluated for the Fe/UV ARP. Also, the combination of ferrous iron and ferric iron should be tested.
2. The effectiveness of UV photolysis at wavelengths other than 254 nm should be tested. Furthermore, other ARP (other combinations of reductants and activating methods) should be investigated for their ability to remove selenocyanate.

REFERENCES

- Airey, P. L.; Dainton, F. S. The Photochemistry of Aqueous Solutions of Fe (II). I. Photoelectron Detachment from Ferrous and Ferrocyanide Ions. Proceedings of the Royal Society of London. Series A. Mathematical and Physical Sciences. **1966**, *291(1426)*: 340-352.
- Analytical Detection Limit Guidance & Laboratory Guide for Determining Method Detection Limits. Wisconsin Department of Natural Resources. Laboratory Certification Program, **1996**.
- Anbar, A. D.; Holland, H. D. The Photochemistry of Manganese and the Origin of Banded Iron Formations. *Geochimica et Cosmochimica Acta*. **1992**, *56(7)*: 2595-2603.
- Balistreri, L. S.; Chao, T. T. Adsorption of Selenium by Amorphous Iron Oxyhydroxide and Manganese Dioxide. *Geochimica et Cosmochimica Acta*. **1990**, *54(3)*: 739-751.
- Betts, R. H.; Dainton, F. S. Electron Transfer and Other Processes Involved in the Spontaneous Bleaching of Acidified Aqueous Solutions of Ferric Thiocyanate. *Journal of the American Chemical Society*. **1953**, *75(22)*: 5721-5727.
- Borowska, Z.; Mauzerall, D. Efficient near Ultraviolet Light Induced Formation of Hydrogen by Ferrous Hydroxide. *Origins of Life and Evolution of the Biosphere*. **1987**, *17(3-4)*: 251-259.
- Burra, R.; Fox, J. D.; Pradenas, G. A.; Vásquez, C. C.; Chasteen, T. G. Biological Interactions of Selenocyanate: Bioprocessing, Detection and Toxicity. *Environmental Technology*. **2009**, *30(12)*: 1327-1335.
- Cameron, C.A.; Davy, E.W. On Some Hitherto Undescribed Compounds of Selenium. *The Transactions of the Royal Irish Academy*. **1881**, *28(2)*: 137-158.
- Chapman, P.M.; Adams, W.J.; Brooks, M.L.; Delos, C.G.; Luoma, S.N.; Maher, W.A.; Ohlendorf, H.M.; Presser, E.S.; Shaw, D.P. Summary of the SETAC Pellston Workshop on Ecological Assessment of Selenium in the Aquatic Environment. Florida, USA. **2009**: 22-28.
- Commandeur, J. M.; Rooseboom, M.; Vermeulen, N. E. Chemistry and Biological Activity of Novel Selenium-Containing Compounds. *Biological Reactive Intermediates VI*. P. Dansette, R. Snyder, M. Delaforge et al, Springer US. **2001**: 105-112.

Crittenden, J.C.; Trussell, R.R.; Hand, D.W.; Howe, K.J.; Tchobanoglous, G. Chemical Oxidation and Reduction. Water Treatment: Principles and Design, Third Edition. **2012**: 457-539.

Crooks, W. Ueber die Selencyanüre. Journal für Praktische Chemie, **1851**, 53: 161–163.

Dogliotti, L.; Hayon, E. Flash Photolysis Study of Sulfite, Thiocyanate, and Thiosulfate Ions in Solution. The Journal of Physical Chemistry. **1968**, 72(5): 1800-1807.

Ehrenreich, A.; Widdel, F. Anaerobic Oxidation of Ferrous Iron by Purple Bacteria, A New Type of Phototrophic Metabolism. Applied and Environmental Microbiology. **1994**, 60(12): 4517-4526.

Golub, A.; Skopenko, V. V. Metal Selenocyanates and Their Properties. Russian Chemical Reviews. **1965**, 34(12): 901-908.

Hayon, E.; Weiss, J. Photochemical Decomposition of Water by Ferrous Ions. Journal of the Chemical Society (Resumed). **1960**, (0): 3866-3872.

Hijnen, W. A. M.; Beerendonk, E. F.; Medema, G. J. Inactivation Credit of UV Radiation for Viruses, Bacteria and Protozoan Cysts in Water: A Review. Water Research. **2006**, 40(1): 3-22.

Kern, W.; Hummel, K. Photosensitive Copolymers of Styrene with 4-Vinylbenzyl Selenocyanate: Synthesis and Comparison with Similar Copolymers. Polymer. **1996**, 37(11): 2055-2059.

Kleinjan, W.E.; Keizer, A.; Janssen, A.J.H. Kinetics of the Chemical Oxidation of Polysulfide Anions in Aqueous Solution. Water Research. **2005**, 39(17): 4093–4100.

Krouse, H. R.; Thode, H. G. Thermodynamic Properties and Geochemistry of Isotopic Compounds of Selenium. Canadian Journal of Chemistry. **1962**, 40(2): 367-375.

Levander, O. A Global View of Human Selenium Nutrition. Annual Review of Nutrition. **1987**, 7(1): 227-250.

Li, W.; Lu, S.; Qiu, Z.; Lin, K. Clofibric Acid Degradation in UV254/H₂O₂ Process: Effect of Temperature. Journal of Hazardous Materials. **2010**, 176(1–3): 1051-1057.

Luria, M.; Treinin, A. Photochemistry of Thiocyanate Ion in Solution. The Journal of Physical Chemistry. **1968**, 72(1): 305-308.

Manceau, A.; Gallup, D. L. Removal of Selenocyanate in Water by Precipitation: Characterization of Copper–Selenium Precipitate by X-ray Diffraction, Infrared, and X-

ray Absorption Spectroscopy. *Environmental Science & Technology*. **1997**, *31(4)*: 968-976.

McNeal, J. M.; Balistrieri, L. S. Geochemistry and Occurrence of Selenium: An Overview. *Selenium in Agriculture and the Environment*. L.W. Jacobs, US. **1989**: 1-13.

Meng, X.; Bang, S.; Korfiatis, G. P. Removal of Selenocyanate from Water Using Elemental Iron. *Water Research*. **2002**, *36(15)*: 3867-3873.

Miekeley, N.; Pereira, R.C.; Casartelli, E.A.; Almeida, A.C.; Carvalho, M. Inorganic Speciation Analysis of Selenium by Ion Chromatography-Inductively Coupled Plasma-Mass Spectrometry and Its Application to Effluents from A Petroleum Refinery. *Spectrochimica Acta Part B: Atomic Spectroscopy*. **2005**, *60(5)*: 633-641.

Murphy, A.P. Removal of Selenate from Water by Chemical Reduction. *Industrial & Engineering Chemistry Research*. **1988**, *27(1)*: 187-191.

Overman, S. D. Apparatus for Removing Selenium from Refinery Process Water and Waste Water Streams. U.S. Patent, **2000**, US6156191 A.

Parida, K.M.; Gorai, B.; Das, N.N.; Rao, S.B. Studies on Ferric Oxide Hydroxides: III. Adsorption of Selenite (SeO_2-3) on Different Forms of Iron Oxyhydroxides. *Journal of Colloid and Interface Science*. **1997**, *185(2)*: 355-362.

Pathem, B.K.; Pradenas, G.A.; Castro, M.E.; Vásquez, C.C.; Chasteen, T.G. Capillary Electrophoretic Determination of Selenocyanate and Selenium and Tellurium Oxyanions in Bacterial Cultures. *Analytical Biochemistry*. **2007**, *364(2)*: 138-144.

Sandy, T.; DiSante, C. Review of Available Technologies for the Removal of Selenium from Water. Prepared for the North American Metals Council. **2010**.

Schrauzer, G.; Guth, T. Hydrogen Evolving Systems. 1. The Formation of Molecular Hydrogen from Aqueous Suspensions of Iron (II) Hydroxide and Reactions with Reducible Substrates, Including Molecular Nitrogen. *Journal of the American Chemical Society*. **1976**, *98(12)*: 3508-3513.

Sedlak, D.L.; Chan, P.G. Reduction of Hexavalent Chromium by Ferrous Iron. *Geochimica et Cosmochimica Acta*. **1997**, *61(11)*: 2185-2192.

Stivanin de Almeida, C. M.; Ribeiro, A.S.; Saint'Pierre, T.D.; Miekeley, N. Studies on the Origin and Transformation of Selenium and Its Chemical Species along the Process of Petroleum Refining. *Spectrochimica Acta Part B: Atomic Spectroscopy*. **2009**, *64(6)*: 491-499.

US. E.P.A. 40 Code of Federal Regulations, Part 136: Analytical Procedures, Appendix B. **2003**.

US. E.P.A. National Recommended Water Quality Criteria-correction. **1999**, EPA 822-Z-99-001. Washington, D.C., US.

US. E.P.A. Draft Aquatic Life Water Quality Criteria for Selenium-2004. **2004**, EPA 822-D-04-001, Washington, D.C., US.

US. E.P.A. 2011 Edition of the Drinking Water Standards and Health Advisories. **2011**, EPA 820-R-11-002, Washington, DC., US.

Watson, M. Selenium Removal Technology Study: Project Final Report. Prepared for Western States Petroleum Association, Concord, California. **1995**.